nature medicine

ARTICLES

https://doi.org/10.1038/s41591-022-01937-6

Individualized, heterologous chimpanzee adenovirus and self-amplifying mRNA neoantigen vaccine for advanced metastatic solid tumors: phase 1 trial interim results

Christine D. Palmer[1], Amy R. Rappaport[1], Matthew J. Davis[1], Meghan G. Hart[1], Ciaran D. Scallan[1], Sue-Jean Hong[1], Leonid Gitlin[1], Lauren D. Kraemer[1], Sonia Kounlavouth[1], Aaron Yang[1], Lindsey Smith[1], Desiree Schenk[1], Mojca Skoberne[1], Kiara Taquechel[1], Martina Marrali[1], Jason R. Jaroslavsky[1], Charmaine N. Nganje[1], Elizabeth Maloney[1], Rita Zhou[1], Daniel Navarro-Gomez[1], Adrienne C. Greene[1], Gijsbert Grotenbreg[1], Renee Greer[1], Wade Blair[1], Minh Duc Cao[1], Shawn Chan[1], Kyounghwa Bae[1], Alexander I. Spira[2], Sameek Roychowdhury[3], David P. Carbone[3], Brian S. Henick[4], Charles G. Drake[4], Benjamin J. Solomon[5], Daniel H. Ahn[6], Amit Mahipal[7], Steve B. Maron[8], Benny Johnson[9], Raphael Rousseau[1], Roman Yelensky[1], Chih-Yi Liao[10], Daniel V. T. Catenacci[10], Andrew Allen[1], Andrew R. Ferguson[1] and Karin Jooss[1]✉

Checkpoint inhibitor (CPI) therapies provide limited benefit to patients with tumors of low immune reactivity. T cell-inducing vaccines hold promise to exert long-lasting disease control in combination with CPI therapy. Safety, tolerability and recommended phase 2 dose (RP2D) of an individualized, heterologous chimpanzee adenovirus (ChAd68) and self-amplifying mRNA (samRNA)-based neoantigen vaccine in combination with nivolumab and ipilimumab were assessed as primary endpoints in an ongoing phase 1/2 study in patients with advanced metastatic solid tumors (NCT03639714). The individualized vaccine regimen was safe and well tolerated, with no dose-limiting toxicities. Treatment-related adverse events (TRAEs) >10% included pyrexia, fatigue, musculoskeletal and injection site pain and diarrhea. Serious TRAEs included one count each of pyrexia, duodenitis, increased transaminases and hyperthyroidism. The RP2D was 10^{12} viral particles (VP) ChAd68 and 30 µg samRNA. Secondary endpoints included immunogenicity, feasibility of manufacturing and overall survival (OS). Vaccine manufacturing was feasible, with vaccination inducing long-lasting neoantigen-specific CD8 T cell responses. Several patients with microsatellite-stable colorectal cancer (MSS-CRC) had improved OS. Exploratory biomarker analyses showed decreased circulating tumor DNA (ctDNA) in patients with prolonged OS. Although small study size limits statistical and translational analyses, the increased OS observed in MSS-CRC warrants further exploration in larger randomized studies.

Cancer immunotherapies have shown promise in harnessing the immune system to target and destroy cancers, leading to clinical benefit enriched in patients with a high mutational burden[1–5]. Multiple studies indicate that cytotoxic CD8 T cells targeting tumor neoantigens are critical to tumor control and clearance in response to immunotherapies targeting CTLA-4 or PD-1[6–10]. Clinical responses to CPI therapy rely mostly on reinvigorating preexisting tumor-specific T cell responses[11], and active vaccination to expand preexisting and prime de novo tumor-specific T cells is anticipated to overcome this limitation.

The limited success of cancer vaccines in the past can be attributed to a number of factors, including selection of poorly immunogenic self-antigens[12], insufficiently immunogenic vaccine platforms and immunosuppressive milieus in patients with advanced cancers[4]. Accordingly, peptide-based neoantigen vaccine platforms have to date failed to consistently induce robust neoantigen-specific CD8 T cell responses in the majority of patients[13–15]. Although more immunogenic, a homologous prime boost messenger RNA (mRNA)-based vaccination approach elicited predominantly CD4 T cell responses[16–18]. Cumulatively, previous findings suggest that a successful cancer vaccine should (1) target tumor-specific neoantigens, (2) use highly immunogenic vaccine platform(s), (3) expand and prime T cells, (4) be combined with CPI therapy[19] and (5) generate long-term memory responses to ensure continuous tumor control for durable clinical benefit.

Viral vector-based vaccine platforms, such as recombinant adenovirus, are able to prime robust T cell responses[20–24]. Although high seroprevalence of anti-adenoviral antibodies in human populations

[1]Gritstone bio, Inc., Emeryville, CA, USA. [2]Virginia Cancer Specialists, Virginia Cancer Specialists, VA, Fairfax, USA. [3]The Ohio State University Medical Center, Columbus, OH, USA. [4]Columbia University Medical Center, New York, NY, USA. [5]Peter MacCallum Cancer Centre, Melbourne, VIC, Australia. [6]Mayo Clinic, Phoenix, AZ, USA. [7]Mayo Clinic Cancer Center, Rochester, MN, USA. [8]Memorial Sloan Kettering Cancer Center, New York, NY, USA. [9]The University of Texas MD Anderson Cancer Center, Houston, TX, USA. [10]University of Chicago Comprehensive Cancer Center, Chicago, IL, USA. ✉e-mail: kjooss@gritstone.com

can lead to diminished immune responses to antigens delivered via adenoviral-based vaccines[20,25], preexisting anti-vector immunity can be circumvented by using non-human adenoviral species, such as chimpanzee adenovirus (ChAd). RNA virus-based vaccines have been tested in humans in a range of cancer and infectious disease indications[26,27], and samRNA vectors are of particular interest due to their ability to express high and durable antigen levels[28].

In this study, the quality of antigen-specific T cell responses induced by a heterologous vaccine regimen consisting of a ChAd vector (ChAd68) and a fully synthetic Venezuelan equine encephalitis virus-based samRNA vector was assessed in non-human primates (NHPs) and patients with advanced cancers in combination with CPIs. The potency and longevity of the immune response against simian immunodeficiency virus (SIV) model antigens[29] and the impact of subcutaneous (s.c.) anti-CTLA-4 administration were assessed in NHPs. Immunogenicity against individualized (patient-specific) predicted cancer neoantigens[30] and in-depth analysis of T cell responses elicited by vaccination are being assessed in an ongoing first-in-human phase 1/2 clinical trial (GRANITE, NCT03639714) in patients with metastatic MSS-CRC, non-small cell lung cancer (NSCLC) or gastroesophageal adenocarcinoma (GEA). Primary endpoints of the phase 1 part of the study were safety and tolerability and RP2D. Secondary and exploratory endpoints include immunogenicity, OS, feasibility of manufacturing patient-specific vaccines and changes in ctDNA. Induction of neoantigen-specific CD8 T cell responses was observed in all patients, including patients with MSS-CRC whose tumors lacked immune reactivity before vaccination. Decreases in ctDNA and stabilization of disease and/or reduction in tumor burden in these patients suggest early signs of potential therapeutic benefit in this CPI-refractory patient population[31–33].

Results

Vaccination induces durable CD8⁺ T cell responses in NHPs. To assess the potency and durability of the immune responses induced by this heterologous vaccine regimen preclinically in NHPs, a model antigen cassette encoding six well-defined NHP-specific MAMU-A*01-restricted SIV antigens[29] was inserted into the ChAd68 and samRNA vaccine platforms. MAMU-A*01-positive rhesus macaques were immunized intramuscularly (i.m.) with ChAd68 prime ($n=11$), followed by i.m. samRNA boosts at 4, 12 and 20 weeks, with ($n=6$) or without ($n=5$) concomitant administration of s.c. anti-CTLA-4 antibody ipilimumab (Fig. 1a and Supplementary Table 1). ChAd68 induced immune responses against all six antigens (mean 923 and 313 spot-forming units (SFU)/10^6 cells at week 4 ± s.c. ipilimumab, respectively; Fig. 1b). Primed T cell responses were boosted following administration of samRNA, with T cell responses still detectable 32 weeks after prime in both groups. Concomitant administration of s.c. ipilimumab resulted in maintenance of an overall higher T cell response (mean 843 and 277 SFU/10^6 cells ± s.c. ipilimumab, respectively; Fig. 1b). ChAd68 readministration at week 32 boosted T cell responses ~15-fold and ~12-fold ± concomitant ipilimumab, respectively (Fig. 1c). Immunization resulted in the generation and maintenance of antigen-specific effector memory T cells (Extended Data Fig. 1a), which have been demonstrated to be predictive of providing therapeutic benefit to patients with cancer[34].

In both therapeutic and prophylactic vaccine settings, the generation and maintenance of long-lived memory responses is highly desirable to maintain disease control or provide protection from future infections. To investigate whether antigen-specific memory T cells were detectable in NHPs up to 2 years after the ChAd68 prime vaccination, six animals that had not received additional treatment and remained available from the initial study were assessed. Tetramer analysis of peripheral blood mononuclear cells (PBMCs) 80 weeks after ChAd68 prime identified the presence of antigen-specific central memory T cells (Extended Data Fig. 1b). Accordingly, interferon-γ (IFN-γ) ELISpot at week 106 revealed positive responses to four or more of the SIV antigens in all six animals, and samRNA administration at week 106 resulted in an ~8-fold and ~17-fold increase in antigen-specific T cell response detectable at week 107 ± s.c. ipilimumab, respectively (Fig. 1d and Extended Data Fig. 1c). Finally, the ability of the boosted antigen-specific CD8 T cells to kill target cells presenting SIV epitopes was determined. CD8 T cells from all six animals showed cytotoxic activity against their cognate targets, with CD8 T cells from four of six animals achieving killing of >70%, even at the lower effector-to-target ratio of 10:1 (Extended Data Fig. 1d).

Individualized vaccine regimen is safe and well tolerated. After establishing the potency and longevity of T cell responses induced by this vaccine in NHPs, the vaccine was assessed as an individualized, heterologous regimen expressing patient-specific neoantigens in an ongoing phase 1/2 clinical study in patients with advanced cancers (Extended Data Fig. 2a; NCT03639714). The primary objectives for the phase 1 portion of this study were assessment of safety, tolerability and RP2D. A single priming dose of ChAd68 was administered i.m. followed by multiple i.m. samRNA boosts with escalating doses of samRNA (Fig. 2a). Eligible patients included those with metastatic MSS-CRC, NSCLC or GEA who were beginning treatment with standard-of-care chemotherapy during vaccine manufacturing and had tissue available for neoantigen prediction, normal organ function and no contraindications for treatment with immunotherapy (Methods). As of data cutoff, enrollment in phase 1 had been completed, and the study is ongoing. For each patient meeting a threshold for cumulative predicted neoantigen score[30] (Extended Data Fig. 2a), the 20 highest ranking mutations were selected for inclusion in a codon-optimized vaccine expression cassette. The same expression cassette was inserted into both patient-specific vaccine vectors for manufacturing. Patient-specific vaccines were successfully manufactured for 15 patients enrolled for vaccine manufacturing, confirming manufacturing feasibility (a secondary endpoint) of this individualized vaccination approach (one patient subsequently elected not to receive study treatment). Fourteen patients received vaccination and monthly intravenous (i.v.) anti-PD-1 antibody nivolumab administration (480 mg every 4 weeks). Patients at dose level 3 (DL3) and DL4 also received s.c. ipilimumab (30 mg) with each vaccination (Fig. 2a and Table 1). Four patients (G1, G8, G9 and G10) received continued standard-of-care chemotherapy with study treatment, and eight patients received a single ChAd68 boost ≥24 weeks after the prime vaccination (Extended Data Table 1). Planned dosing intervals and timepoints with blood draws for immunogenicity are shown in Extended Data Fig. 2b. The median age of the 14 phase 1 patients was 59 years; tumor types included metastatic MSS-CRC ($n=7$), GEA ($n=6$) or NSCLC ($n=1$); and patients had received one or two prior lines of therapy (Table 1 and Extended Data Table 1). The individualized vaccine regimen was safe and well tolerated, with no dose-limiting toxicities. The primary safety endpoint of this vaccine regimen was reflective of a viral-based vaccine regimen with TRAEs consistent with a vaccine-induced immune response (Fig. 2b). TRAEs >10% included pyrexia (86%), fatigue (43%), musculoskeletal and injection site pain (both 36%) and diarrhea (29%). Serious TRAEs were largely consistent with the known safety profile of CPI therapy and included one count each of pyrexia, duodenitis, increased transaminases and hyperthyroidism (Fig. 2b). Based on the totality of the safety and immunogenicity data (secondary endpoint; see next section) from the phase 1 part of the study, the primary endpoint of RP2D was determined to be 10^{12} VP ChAd68 and 30 μg samRNA.

Vaccine induces neoantigen-specific CD8⁺ T cells. The key secondary endpoint of immunogenicity was assessed for neoantigen-specific T cells. To preferentially stimulate CD8 T cells

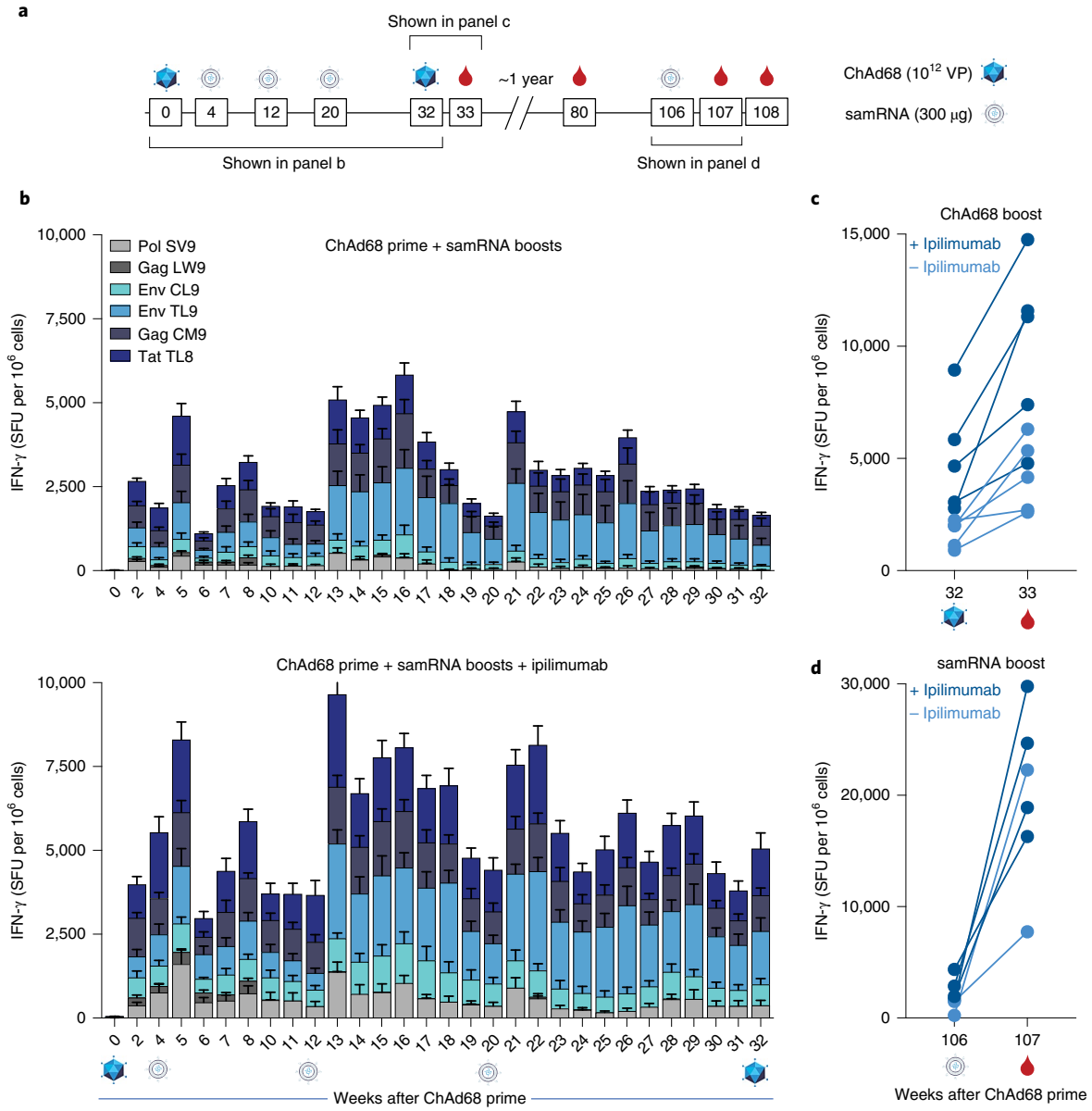

Fig. 1 | Heterologous vaccination with ChAd68 and samRNA induces broad, durable CD8⁺ T cell responses in NHPs that are detectable long-term and can be boosted ≥2 years after prime. a, Schematic of study treatment schedule. **b**, Antigen-specific T cell response (IFN-γ SFU per 10^6 cells) at each measured timepoint for duration of study for each group (mean ± standard error of the mean for each antigen stacked), $n=6$ per group up to week 20 ($n=5$ for group without ipilimumab at weeks 24–107; Supplementary Table 1). **c**, Antigen-specific T cell response at weeks 32 and 33 (before and after ChAd68 boost) for each group ($n=5$ without ipilimumab, $n=6$ with ipilimumab), average response per animal (SFU per 10^6 cells) for all antigens stacked. **d**, Antigen-specific T cell response at weeks 106 and 107 (before and after samRNA boost) for each group ($n=5$ without ipilimumab, $n=6$ with ipilimumab), average response per animal (SFU per 10^6 cells) for all antigens stacked.

via major histocompatibility complex (MHC) class I presentation in immune assays[30,35,36], individual patient minimal epitope (8–11mer) peptide pools were designed to include the 40 highest ranked predicted neoepitopes (CD8 pool; Supplementary Table 2). Because this exploratory minimal epitope pool design does not include all potential neoantigens per mutation and can disproportionately favor some mutations with high prediction scores, additional patient-specific peptide pools consisting of overlapping 15mers spanning each vaccine cassette were also used to interrogate T cell responses more broadly (15mer pool; Supplementary Table 2). Posttreatment PBMC samples were available for 13 of 14 patients (all except patient G5). Stimulation of PBMCs with patient-specific peptide pools resulted in IFN-γ responses detectable by ex vivo ELISpot following heterologous prime boost vaccination in 100% of patients (13/13), with a ChAd68 boost further increasing peripheral T cell levels in 67% of patients (4/6) with evaluable post-boost samples (Fig. 2c and Extended Data Fig. 3a). Only 15% of patients (2/13) had responses above LOD to their cognate neoantigen peptide pool at baseline, which were increased following vaccine administration (Fig. 2c). Similarly to observations in NHPs, vaccine-induced T cell responses were long-lived, and T cell levels of 700–5,000 SFU/10^6 cells were maintained for >52 weeks in three patients with available longitudinal samples (Extended Data Fig. 3a,b). Notably, readministration of ChAd68 resulted in elevated T cell levels detectable 12–24 weeks after ChAd68 boost (patients G1, G3, G8 and G11; Fig. 2b and Extended Data Fig. 3a). Dose escalation

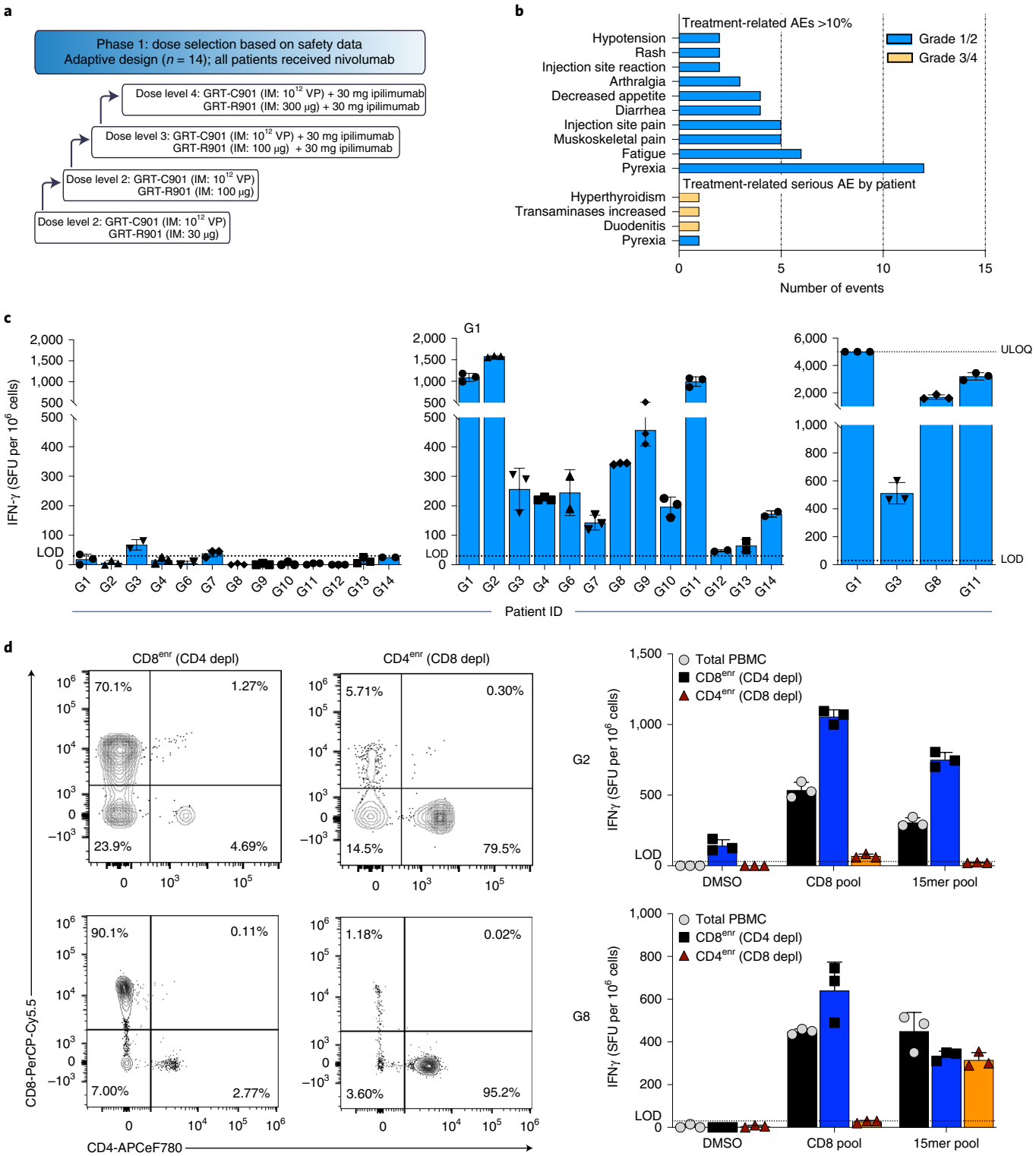

Fig. 2 | First-in-human data show the vaccine regimen is safe and induces CD8⁺ T cell responses against predicted patient-specific cancer neoantigens. **a**, Phase 1 study schematic outlining dose escalation. **b**, Safety data: TRAEs >10% and all treatment-related serious adverse events (AEs) are shown ($n = 14$ patients). Graph shows counts of grade 1/2 (blue bars) and 3/4 (orange bars) events. **c**, Patient PBMC ex vivo IFN-γ ELISpot responses to patient-specific peptide pools (Supplementary Table 2) are shown for baseline (left panel), maximum response following ChAd prime and samRNA boosts (middle panel) and maximum response post ChAd boost (right panel). Graphs show mean SFU per 10^6 PBMCs ± standard deviation (s.d.) for triplicate ELISpot wells. Assay limit of detection (LOD) and upper limit of quantitation (ULOQ) are indicated by dotted lines. **d**, Flow plot showing relative CD8 and CD4 T cell frequencies in CD4- or CD8-depleted (depl) PBMC populations. Corresponding ELISpot data (mean SFU of technical replicates ± s.d.) are shown for whole PBMCs (black bars), $CD8^{enr}$ PBMCs (navy blue bars) and $CD4^{enr}$ PBMCs (orange bars) stimulated with dimethylsulfoxide (DMSO), patient-specific CD8 or 15mer pools for patients G2 and G8.

Table 1 | Baseline and disease characteristics by DL

	DL1 (*n* = 3)	DL2 (*n* = 2)	DL3 (*n* = 3)	DL4 (*n* = 6)	Total (*n* = 14)
Age (yr), median (range)	72 (59–74)	70 (63–76)	51 (50–53)	55 (38–61)	59 (38–76)
Female gender, *n* (%)	1 (33)	1 (50)	1 (33)	1 (17)	4 (29)
ECOG, *n* (%)					
0	2 (67)	1 (50)	1 (33)	3 (50)	7 (50)
1	1 (33)	1 (50)	2 (67)	3 (50)	7 (50)
Number of prior therapies, *n* (%)					
1	2 (67)	1 (50)	1 (33)	2 (33)	6 (43)
2	1 (33)	1 (50)	2 (67)	4 (67)	8 (57)
Prior anti-PD(L)1 therapy, *n* (%)					
Yes	1 (33)	0 (0)	0 (0)	0 (0)	1 (7)
No	2 (67)	2 (100)	3 (100)	6 (100)	13 (93)
Tumor types, *n* (%)					
MSS-CRC	0	1 (50)	2 (67)	4 (67)	7 (50)
GEA	2 (67)	1 (50)	1 (33)	2 (33)	6 (43)
NSCLC	1 (33)	0	0	0	1 (7)

DL1, GRT-C901/GRT-R902 30 μg + i.v. nivolumab; DL2, GRT-C901/GRT-R902 100 μg + i.v. nivolumab; DL3, GRT-C901/GRT-R902 100 μg + i.v. nivolumab + s.c. ipilimumab; DL4, GRT-C901/GRT-R902 300 μg + i.v. nivolumab + s.c. ipilimumab. ECOG, Eastern Cooperative Oncology Group.

of samRNA suggested that more consistent boosts in T cell responses were observed in patients receiving 30-μg and 100-μg doses of samRNA (Extended Data Fig. 3c). Prolonged samRNA dosing intervals of 8–16 weeks occurring due to logistical constraints during coronavirus disease 2019 (COVID-19) restrictions revealed interesting insights into the kinetics of samRNA-boosted T cell responses (Extended Data Fig. 3a,b). In patient G1 (GEA, concomitant chemotherapy), T cells expanded 1.5-fold during an 8-week interval between samRNA boosts and remained consistently >700 SFU/10^6 cells during a 16-week period following samRNA administration at week 52. A sevenfold increase in CD8 T cell responses between samRNA doses at weeks 24 and 36 was observed in patient G3 (NSCLC). Patient G2 (GEA) T cell responses showed ~1.5-fold contractions and expansions of the T cell response during a 9-week samRNA dosing interval between weeks 4 and 13. These data suggested that lower doses and longer boost intervals may be beneficial in driving T cell responses with this new samRNA platform. This led to the selection of 30 μg samRNA as the RP2D, a primary endpoint (see previous section) and longer boost intervals (8 weeks) being assessed in the ongoing phase 2 part of this study.

CD8⁺ T cells recognize neoantigens in multiple HLA alleles. Responses to cognate CD8 pools and 15mer pools were analyzed for CD8 versus CD4 T cell bias in five patients with available samples (G1, G2, G8, G11 and G14). As expected based on peptide length, IFN-γ responses following CD8 pool stimulation were driven by CD8 T cells, whereas responses to 15mer pool stimulation were either CD8-driven or mixed CD4/CD8 T cell responses (Fig. 2d, Extended Data Fig. 4a). Active vaccination against tumor neoantigens should lead to expansion of preexisting and priming of *de novo* tumor-specific T cell responses. To assess the breadth of responses with limited available PBMC samples, 4 minipools covering the 20 patient-specific vaccine neoantigens (Supplementary Table 2) were used to partially deconvolute T cell responses in 12 of 13 patients. Positive responses to four different minipools indicate responses to at least four different mutations. Antigen-specific expansion of T cells in short in vitro stimulation (IVS) cultures[30,37] confirmed expansion of preexisting and priming of de novo T cell responses after treatment (Extended Data Fig. 4b). All 12 patients tested had detectable T cell responses to multiple mutations at post-treatment timepoints (Fig. 3a). Voluntary leukapheresis and pooled posttreatment timepoints enabled full deconvolution of T cell responses against all 40 minimal epitopes included in the CD8 pool for patients G1, G2 and G8, revealing positive responses to ≥50% of vaccine mutations in multiple HLA class I alleles for all three patients (Fig. 3b,c and Extended Data Fig. 5). These data indicate that partial deconvolution via minipools (often necessitated due to limitations in sample availability) likely underestimates the true breadth of neoantigen-specific responses induced by this heterologous vaccine. Peptide-HLA (pHLA) tetramers were generated to assess the breadth and memory phenotype of antigen-specific T cells. pHLA binding was detected in the context of multiple HLA class I alleles for patients G1, G2 and G8. Tetramer-positive CD8 T cells were characterized by 1.3- to 1.5-fold higher frequencies of effector memory and up to 20-fold lower frequencies of naive T cells when compared to total CD8 T cells (Fig. 3d and Extended Data Fig. 6a). ChAd68 boost in patient G1 resulted in a 10-fold increase in tetramer positive cells, with post-boost tetramer-positive CD8 T cells consisting of ≥93% effector memory cells in the context of both class I alleles tested (Fig. 3e and Extended Data Fig. 6b).

CD8⁺ T cells are polyfunctional and kill target cells. In addition to driving broad T cell responses, a potent vaccine regimen should induce cytotoxic T cells that are able to kill target cells presenting cognate epitopes in the context of MHC class I. Secretion of cytotoxic markers assessed by Meso Scale Discovery (MSD) and triplex FluoroSpot was confirmed in eight patients (Extended Data Fig. 6c,d). Notably, readministration of ChAd68 resulted in increased granzyme B secretion following CD8 pool stimulation in four of six patients with evaluable post-ChAd68 boost timepoints (Extended Data Fig. 6e). To assess whether this cytotoxic signature was driven by CD8 T cells, cytokine secretion was analyzed via intracellular cytokine staining (ICS). Stimulation of ex vivo PBMCs with CD8 pool resulted in detectable frequencies of IFN-γ⁺, CD107α⁺, tumor necrosis factor α (TNF-α)⁺ and interleukin-2 (IL-2)⁺ CD8 T cells in patients G2 and G8, which were increased ~2-fold to ~700-fold following IVS expansion (Fig. 4a and Extended Data Fig. 7a). Boolean gating confirmed the presence of quadruple-, triple-, and double-positive polyfunctional CD8 T cells for both patients (Fig. 4b, Extended Data Fig. 7b). Polyfunctional CD4 T cell responses following cognate 15mer pool stimulation were also detectable in patients G2 and G8 following IVS culture (Extended Data Fig. 7c). The ability of antigen-specific CD8 T cells to kill target cells presenting neoantigen was determined. Co-culture of expanded neoantigen-specific patient T cells with single HLA allele-expressing target cells pulsed with cognate neoantigen peptides resulted in a 2.5-fold to 6.4-fold decrease in live target cells over time compared to controls, indicating antigen-specific T cell-driven killing of target cells presenting cognate pHLA for both patients G2 and G8 (Fig. 4c and Extended Data Fig. 7d).

T cells are increased in tumors following vaccination. To exert anti-tumor effects and clinical benefit in patients, vaccine-induced T cells need to infiltrate tumors and lyse cells presenting their cognate pHLA antigen through recognition via the T cell receptor (TCR). Paired TCR sequencing and gene expression profiling via single-cell RNA sequencing was performed on baseline and on-treatment PBMC timepoints from patients with available corresponding tumor biopsies (G1 and G3; Extended Data Fig. 8a). Neoantigen-reactive CD8 T cells were increased 1.6-fold to 6.4-fold in on-treatment samples compared to baseline (Extended Data Fig. 8b).

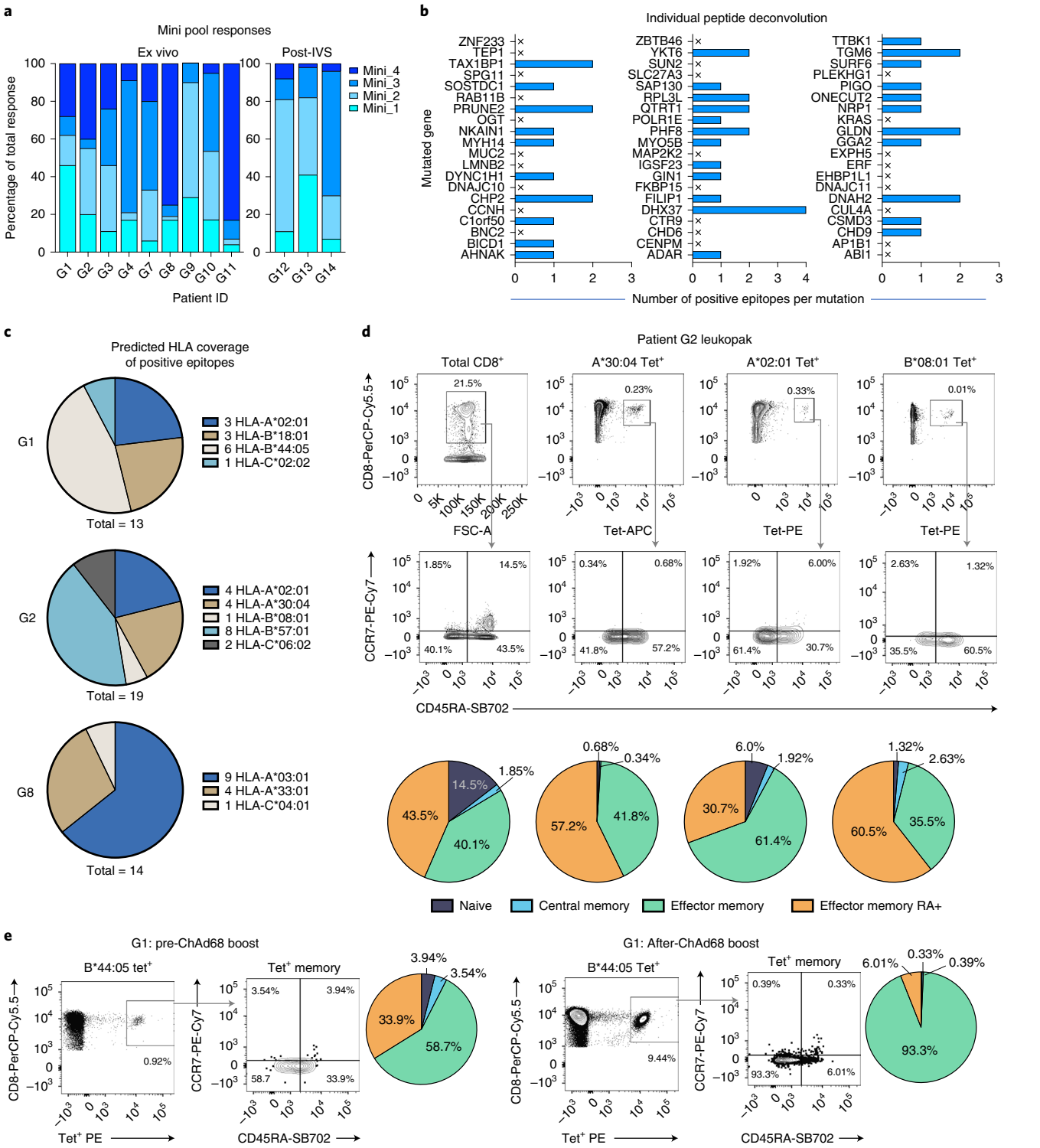

Fig. 3 | Vaccine induces polyclonal effector memory CD8 T cell responses across multiple neoantigens and HLAs. a, Patient PBMCs from available posttreatment timepoints (G1 W12, G2 W5, G3 W8, G4 W6, G7 W4, G8 W12, G9 W8, G10 W16, G11 W16, G12 W12, G13 W12, G14 W13 and G15 W12) were stimulated overnight in ex vivo or post-IVS IFN-γ ELISpot with patient-specific minipools or DMSO. Graphs show percentage of total response of mean IFN-γ responses to minipool 1 (turquoise), minipool 2 (light blue), minipool 3 (medium blue) and minipool 4 (navy blue) for each patient. **b**, Number of positive minimal epitopes detected (positive by ex vivo or post-IVS ELISpot) for each mutated gene. Undetectable responses against epitopes tested are indicated by 'x'. **c**, Pie charts showing patient-specific predicted HLA class I presentation of positive neoantigen responses shown in panel b. **d**, Density plots showing recognition of pHLA (A*30:04, A*02:01, B*08:01) and corresponding T cell memory phenotypes for patient G2. Pie charts showing frequencies of naive ($CD45RA^+CCR7^+$; purple), central memory (CM; $CD45RA^-CCR7^+$; blue), effector memory (EM; $CD45RA^-CCR7^-$; green) and T effector memory RA^+ (TEMRA; $CD45RA^+CCR7^-$; orange) cells in total $CD8^+$ population (left-most chart) and $CD8^+$tetramer$^+$ populations from corresponding dot plots. **e**, Density plots and corresponding pie charts showing recognition of pHLA (B*44:05) and corresponding T cell memory phenotypes before and after ChAd68 boost for patient G1.

Analysis of transcriptional activation signatures confirmed an enrichment for CD8 T cells in on-treatment samples (Extended Data Fig. 8c). TCR analysis revealed a total of 12 and 30 distinct TCR clonotypes (α-β pairs) detected in PBMCs following vaccination for patients G1 and G3, respectively (Extended Data Fig. 8b). Analysis of *IFNG*, *GZMB*, *TNFA* and *IL2* transcripts in T cell clonotypes revealed 12- to 98-fold increases in frequencies of T cells expressing two or more cytokine transcripts in on-treatment samples compared to baseline for both patients (Extended Data Fig. 8d,e and Supplementary Table 3). Baseline and on-treatment tumor biopsy samples from patients G1 and G3 were analyzed for the presence of TCR-β CDR3 sequences via bulk DNA sequencing. Analysis of TCR-β CDR3 sequences obtained independently via single-cell RNA sequencing in PBMCs versus DNA sequencing in tumor samples indicated overlap of putative neoantigen-specific T cells in both the blood and tumor. For patient G1, 341 TCR-β CDR3 clonotypes were identified across baseline and on-treatment tumor samples with an enrichment of nine clones in the on-treatment biopsy. Two of these nine clonotypes were also found in PBMCs sampled at the time of the on-treatment biopsy (Fig. 4d). In patient G3, a total of 294 TCR-β CDR3 clonotypes were identified via DNA sequencing in both tumor samples, with 40 clonotypes enriched in the on-treatment sample. Five of the 40 TCR-β CDR3 clonotypes enriched in the on-treatment biopsy overlapped with the activated TCR clonotypes in PBMCs at the time of the on-treatment biopsies (Fig. 4d). Representation of clonotypes from neoantigen-specific CD8 T cells in tumor tissue that were also detected in PBMCs provides proof-of-concept that vaccine-induced neoantigen-specific T cells in the periphery are able to infiltrate tumors.

Prolonged survival and decreases in ctDNA in MSS-CRC. Multiple measures of activity were assessed, including OS and changes in tumor size via imaging (objective response rate and progression-free survival per RECIST v1.1, all secondary endpoints), as well as transcriptional profiling and changes in ctDNA (both exploratory endpoints). Standard genomic correlates of responsive tumors to CPIs (namely, tumor mutational burden, *CD274* (PD-L1) and *IFNG* RNA sequencing signatures) were analyzed in patient pretreatment biopsies and compared to relevant cancer types from The Cancer Genome Atlas (TCGA). Pretreatment patient genomic data demonstrate that patients with MSS-CRC and GEA in this study had low tumor mutational burden and PD-L1 expression and that these tumors had low immune reactivity (Fig. 5a,b and Supplementary Table 4). Such cold tumors are known to be refractory to CPI therapy. Objective response rate and progression-free survival per RECIST v1.1 show a patient with GEA with a complete response and several patients across tumor types with stable disease (SD) (Extended Data Table 1). Given the observation of SD in several patients with MSS-CRC, we focused on analyzing these seven patients with MSS-CRC for the secondary endpoint of OS and an exploratory endpoint of changes in ctDNA from baseline (Extended Data Table 1 and Supplementary Table 4). For patients with MSS-CRC, 3 of 7 (42.9%) remained alive (median OS of 8.7 months; Extended Data Table 1), with an OS rate at 12 months of 42.9% reflecting multiple patients experiencing durable benefit.

Emerging evidence suggests changes in ctDNA levels on-treatment relative to baseline are a useful biomarker to stratify patients as molecular responders or nonresponders and differentiate patients with a good prognosis, especially those with SD per RECIST v1.1 criteria[38]. Of these patients, 100% (3/3) with treatment durations <6 months had increases in ctDNA concentration, whereas 75% of patients (3/4) with treatment durations ≥6 months demonstrated a molecular response (<50% from baseline; Fig. 5c and Supplementary Table 4). Two patients had complete ctDNA clearance while on treatment (G8 and G14; Fig. 5c). Most notably, these decreases in ctDNA were more frequent in patients with prolonged OS (median OS not reached versus 7.8 months; Fig. 5d). Patient G8, a 51-year-old patient with MSS-CRC who received chemotherapy for 21 months, had progressed on first-line chemotherapy before study treatment initiation but continued concomitant standard of care chemotherapy during study treatment (Extended Data Table 1) and showed clear evidence of tumor regression following vaccine administration via both ctDNA and radiologic assessments. Computed tomography scans showed size reduction in multiple lung lesions within 16 weeks and persistent reduction in multiple lung and one liver lesion through 48 weeks (Fig. 5e). Fluorodeoxyglucose-positron emission tomography imaging of the stable liver lesions showed a lack of hypermetabolic cells following study treatment administration, suggesting anti-tumor activity of this vaccine regimen not evidenced by computed tomography imaging (Fig. 5e). In totality, the safety, immunogenicity, OS and ctDNA signals observed in this trial warrant further investigation of this vaccine platform in patient populations that are refractory to CPI monotherapy[31–33].

Discussion

The quality of antigen-specific T cell responses induced by a heterologous vaccine regimen, consisting of ChAd68 and samRNA vectors in combination with CPI, was assessed in NHPs and patients with advanced cancers. The potency and longevity of T cell responses to model antigens following vaccination were studied in NHPs, whereas safety, immunogenicity and feasibility of an individualized patient-specific vaccine were assessed in patients with late-stage cancer. This vaccine regimen was well tolerated and induced neoantigen-specific CD8 T cell responses in all patients. Vaccine-driven T cell responses were (1) polyclonal across multiple mutations and HLA alleles, (2) polyfunctional and (3) able to kill target cells presenting cognate peptide. Of note, more consistent boosts in T cell responses were observed in patients receiving lower doses of samRNA. This could be due to less innate immune activation via mRNA-sensing pattern recognition receptors that might interfere with samRNA amplification and antigen expression. Increased

Fig. 4 | Neoantigen-reactive CD8 T cells are polyfunctional, kill targets presenting cognate peptides in multiple HLA alleles and are increased in on-treatment tumor samples. a, Representative density plots for patient G2 ICS for CD8$^+$ cells producing IFN-γ, CD107α, TNF-α and IL-2 in ex vivo or IVS-expanded PBMCs stimulated overnight with DMSO or patient-specific CD8 pool. Cells were gated on PBMCs (forward scatter (FSC)-A versus side scatter (SSC)-A), singlets (FSC-A versus FSC-H), live cells (FSC-A versus Live/Dead), CD8 or CD4 T cells (CD8 versus CD4) and cytokine$^+$ cells. **b**, Polyfunctionality was assessed via Boolean gating of CD8$^+$cytokine$^+$ populations (background subtracted). Pie charts show polyfunctionality of ex vivo PBMCs and post-IVS PBMCs. Pie arcs depict individual cytokines in red (CD107α), lime green (IFN-γ), turquoise (TNF-α) and navy blue (IL-2). Pie sections depict frequencies of cells expressing multiple cytokines as outlined in pie category legend. Main functional pie slices are colored red (quadruple positive for CD107α, IFN-γ, TNF-α and IL-2), orange (triple positive for CD107α, IFN-γ and TNF-α) and yellow (double positive for CD107α and IFN-γ). **c**, Target cell killing by IVS-expanded PBMCs from patients G2 (B*08:01, B*57:01, A*30:04). Graphs show relative viability based on NucRed count and normalized to effector-to-target ratio of 10:1 DMSO control over time. Data are shown as mean ± s.d. from duplicate wells for targets alone stimulated with DMSO (gray circles) or cognate peptide (black squares) and for 10:1 effector/target co-cultures stimulated with DMSO (light blue circles) or cognate peptide (navy blue squares). **d**, DNA sequencing of TCR-β chains in tumor samples in baseline and on-treatment samples from patients G1 and G3. TCR-β chains expanded in PBMCs, in both PBMCs and tumors, and contracted are shown.

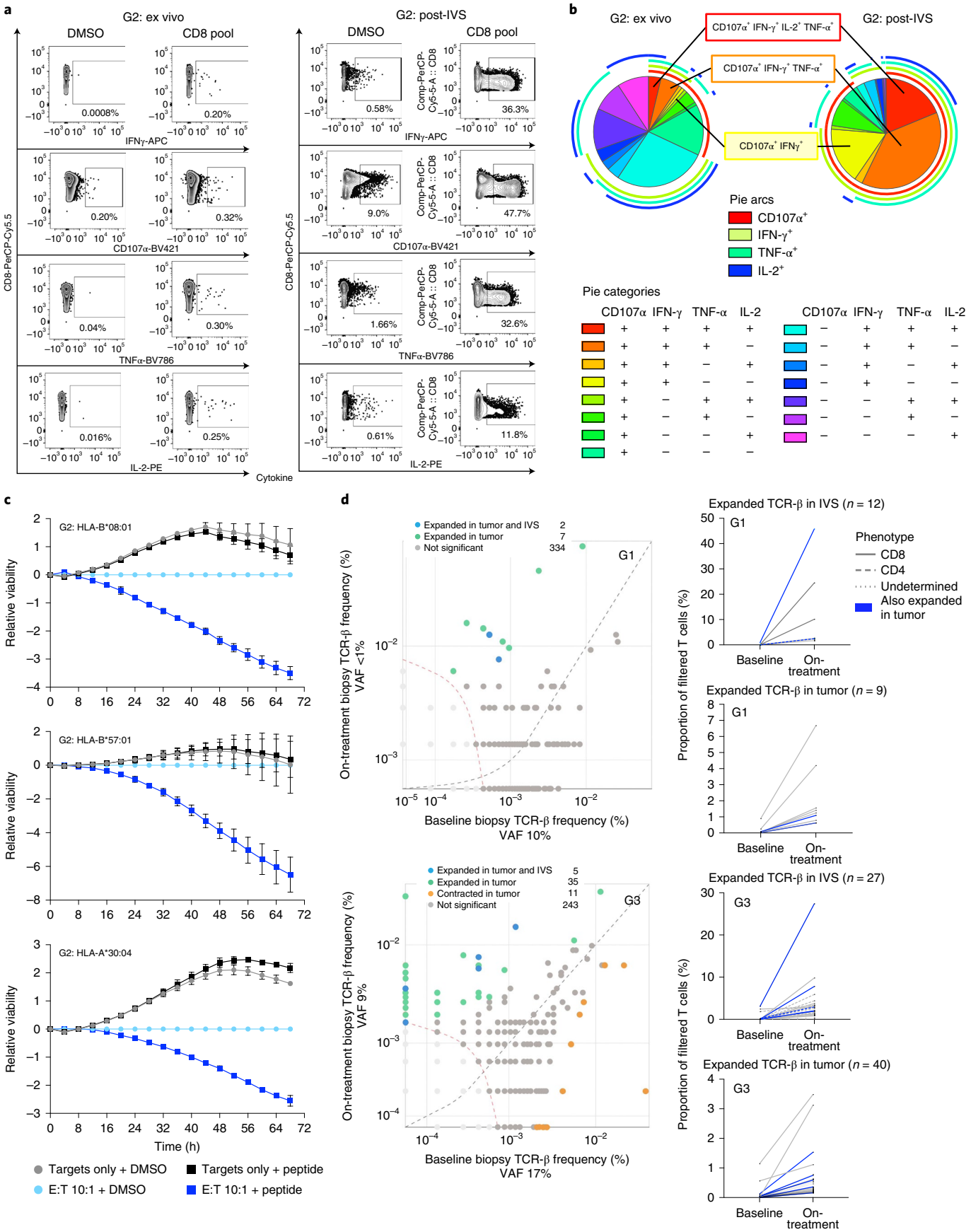
a
G2: ex vivo
G2: post-IVS
DMSO
CD8 pool
0.0008%
0.20%
0.58%
36.3%
0.20%
0.32%
9.0%
47.7%
0.04%
0.30%
1.66%
32.6%
0.016%
0.25%
0.61%
11.8%
IFNγ-APC
CD107α-BV421
TNFα-BV786
IL-2-PE
CD8-PerCP-Cy5.5
Comp-PerCP-Cy5-5-A :: CD8
Cytokine
b
G2: ex vivo
G2: post-IVS
CD107α+ IFN-γ+ IL-2+ TNF-α+
CD107α+ IFN-γ+ TNF-α+
CD107α+ IFNγ+
Pie arcs
CD107α+
IFN-γ+
TNF-α+
IL-2+
Pie categories
CD107α IFN-γ TNF-α IL-2
c
G2: HLA-B*08:01
G2: HLA-B*57:01
G2: HLA-A*30:04
Relative viability
Time (h)
Targets only + DMSO
Targets only + peptide
E:T 10:1 + DMSO
E:T 10:1 + peptide
d
Expanded in tumor and IVS
Expanded in tumor
Contracted in tumor
Not significant
G1
G3
On-treatment biopsy TCR-β frequency (%) VAF <1%
Baseline biopsy TCR-β frequency (%) VAF 10%
On-treatment biopsy TCR-β frequency (%) VAF 9%
Baseline biopsy TCR-β frequency (%) VAF 17%
Expanded TCR-β in IVS (n = 12)
Expanded TCR-β in tumor (n = 9)
Expanded TCR-β in IVS (n = 27)
Expanded TCR-β in tumor (n = 40)
Proportion of filtered T cells (%)
Baseline
On-treatment
Phenotype
CD8
CD4
Undetermined
Also expanded in tumor

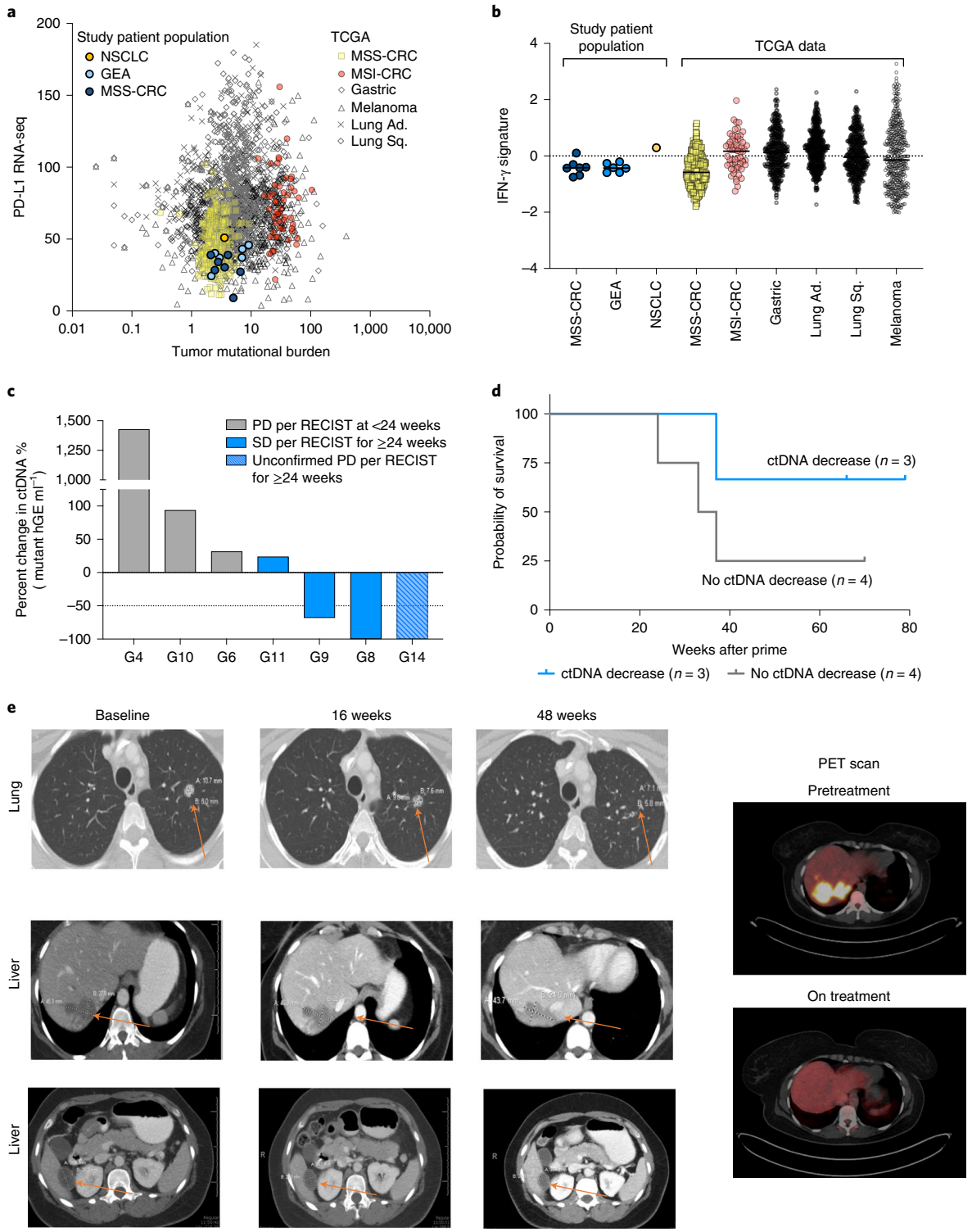

Fig. 5 | Early signals of clinical efficacy in patients with MSS-CRC in advanced disease setting. a, Scatter plot showing tumor sample RNA sequencing (RNA-seq) for patients before study treatment. PD-L1 normalized RNA-sequencing expected counts (*y* axis) versus tumor mutational burden (*x* axis) for patients and relevant TCGA cancer types. **b**, Patient RNA-sequencing IFN-γ signature average z-scores (*x* axis) calculated across patients and relevant TCGA cancer types (*y* axis). TCGA samples: MSS-CRC ($n=286$), MSI-CRC ($n=62$), gastric ($n=406$), lung adenocarcinoma (Lung Ad.)_ ($n=498$), lung squamous (Lung Sq.) ($n=463$) and melanoma ($n=436$). GRANITE patients: MSS-CRC ($n=7$), GEA ($n=6$) and NSCLC ($n=1$). **c**, Percent change in ctDNA following initiation of study treatment relative to baseline levels shown as best response and colored by RECIST-based response and time on treatment. Patients in blue were all on study treatment >24 weeks with two patients treated beyond RECIST-based progressive disease (PD) that was not confirmed by 24 weeks and continued on study treatment. **d**, Probability of survival in MSS-CRC patients with ($n=4$) or without ($n=3$) reduction in ctDNA since ChAd68 prime. Data cutoff 31 January 2022. **e**, Radiological images showing tumor lesions in the lung and liver of patient G8 before initiating study treatment (baseline) and following study treatment (16 and 48 weeks). Fluorodeoxyglucose-positron emission tomography imaging of tumor lesions in the liver when patient was diagnosed in February 2018 and 7 months after starting study treatment. Arrows indicate relevant target lesions.

frequencies of vaccine-induced TCR clonotypes were found in on-treatment tumor samples, providing proof-of-concept for tumor infiltration of vaccine-induced T cells. Patients with molecular responses following vaccination showed stabilization and/or reduction of target lesions and prolonged OS, indicating potential early signs of clinical activity in this CPI-refractory patient population. A randomized phase 2/3 study has been initiated to demonstrate the efficacy of this vaccine regimen in patients with MSS-CRC in the first-line metastatic setting (NCT05141721).

A vaccine that induces neoantigen-specific CD8 T cells provides a foundation for combination with CPIs, making their combined administration highly desirable. Although the effects of s.c. ipilimumab were difficult to discern in this small cohort of patients, administration of ipilimumab in addition to a vaccine in NHPs resulted in increased breadth and magnitude of antigen-specific T cell responses in all animals. This may be due to a lower threshold for T cell activation against weaker epitopes with ipilimumab compared to vaccine alone. The lower threshold of T cell activation provided by the addition of ipilimumab might allow induction of an overall broader immune response to vaccine-encoded neoantigens and a more robust immune attack of the tumor. Driving broad T cell responses against multiple tumor antigens across multiple HLA alleles, as observed in this study, may limit the impact of common HLA-related immune escape mechanisms[39–41]. As a patient's disease progresses, increased heterogeneity can lead to immune evasion. Treating patients earlier in their disease, such as in the adjuvant setting or early in the treatment of metastatic disease, has the potential benefit of completely eradicating tumor cells by vaccine-induced T cells before resistance mutations arise. Also, given the time lag between vaccine administration and T cell expansion, patients with lower initial disease burden and more time to generate a T cell response before disease progression are more likely to receive long-term benefit and durable disease control from our vaccination approach. Increasing evidence suggests that a clear survival benefit (even without a radiologic response) may be a hallmark of immunotherapies[42]. Follow-up of this ongoing phase 1/2 study is ongoing, and one phase 2/3 and one phase 2 study are assessing potential clinical activity of this vaccine regimen in patients with MSS-CRC in the metastatic and adjuvant treatment settings, respectively. In addition to benefiting patients with cancer, this versatile and potent vaccine can be applied to other indications such as prophylactic vaccination against SARS-CoV-2 (ref. [43]) (NCT05148962, NCT04776317). In sum, this versatile heterologous vaccine regimen generates strong, persistent and functional immune responses that have broad applicability to a wide range of disease settings and support continued exploration in the clinical setting to bring better treatment options to patients with cancer and people at risk of infection.

Online content

Any methods, additional references, Nature Research reporting summaries, source data, extended data, supplementary information, acknowledgements, peer review information; details of author contributions and competing interests; and statements of data and code availability are available at https://doi.org/10.1038/s41591-022-01937-6.

Received: 4 March 2022; Accepted: 6 July 2022;
Published online: 15 August 2022

References

1. Lawrence, M. S. et al. Mutational heterogeneity in cancer and the search for new cancer-associated genes. *Nature* **499**, 214–218 (2013).
2. Rizvi, N. A. et al. Cancer immunology. Mutational landscape determines sensitivity to PD-1 blockade in non-small cell lung cancer. *Science* **348**, 124–128 (2015).
3. Snyder, A. et al. Genetic basis for clinical response to CTLA-4 blockade in melanoma. *N. Engl. J. Med.* **371**, 2189–2199 (2014).
4. Lee, C. H., Yelensky, R., Jooss, K. & Chan, T. A. Update on tumor neoantigens and their utility: why it is good to be different. *Trends Immunol.* **39**, 536–548 (2018).
5. Tran, E., Robbins, P. F. & Rosenberg, S. A. 'Final common pathway' of human cancer immunotherapy: targeting random somatic mutations. *Nat. Immunol.* **18**, 255–262 (2017).
6. DuPage, M., Mazumdar, C., Schmidt, L. M., Cheung, A. F. & Jacks, T. Expression of tumour-specific antigens underlies cancer immunoediting. *Nature* **482**, 405–409 (2012).
7. Gubin, M. M. et al. Checkpoint blockade cancer immunotherapy targets tumour-specific mutant antigens. *Nature* **515**, 577–581 (2014).
8. Lennerz, V. et al. The response of autologous T cells to a human melanoma is dominated by mutated neoantigens. *Proc. Natl Acad. Sci. USA* **102**, 16013–16018 (2005).
9. Matsushita, H. et al. Cancer exome analysis reveals a T-cell-dependent mechanism of cancer immunoediting. *Nature* **482**, 400–404 (2012).
10. Robbins, P. F. et al. Mining exomic sequencing data to identify mutated antigens recognized by adoptively transferred tumor-reactive T cells. *Nat. Med.* **19**, 747–752 (2013).
11. Tumeh, P. C. et al. PD-1 blockade induces responses by inhibiting adaptive immune resistance. *Nature* **515**, 568–571 (2014).
12. McGranahan, N. & Swanton, C. Neoantigen quality, not quantity. *Sci. Transl. Med.* **11**, eaax7918 (2019).
13. Keskin, D. B. et al. Neoantigen vaccine generates intratumoral T cell responses in phase Ib glioblastoma trial. *Nature* **565**, 234–239 (2019).
14. Ott, P. A. et al. An immunogenic personal neoantigen vaccine for patients with melanoma. *Nature* **547**, 217–221 (2017).
15. Ott, P. A. et al. A phase Ib trial of personalized neoantigen therapy plus anti-PD-1 in patients with advanced melanoma, non-small cell lung cancer, or bladder cancer. *Cell* **183**, 347–362.e324 (2020).
16. Sahin, U. et al. Personalized RNA mutanome vaccines mobilize poly-specific therapeutic immunity against cancer. *Nature* **547**, 222–226 (2017).
17. Sahin, U. et al. An RNA vaccine drives immunity in checkpoint-inhibitor-treated melanoma. *Nature* **585**, 107–112 (2020).
18. Hilf, N. et al. Actively personalized vaccination trial for newly diagnosed glioblastoma. *Nature* **565**, 240–245 (2019).
19. Riaz, N. et al. Tumor and microenvironment evolution during immunotherapy with nivolumab. *Cell* **171**, 934–949 e916 (2017).
20. Shaw, A. R. & Suzuki, M. Immunology of adenoviral vectors in cancer therapy. *Mol. Ther. Methods Clin. Dev.* **15**, 418–429 (2019).
21. Lopez-Camacho, C. et al. Rational Zika vaccine design via the modulation of antigen membrane anchors in chimpanzee adenoviral vectors. *Nat. Commun.* **9**, 2441 (2018).
22. Ogwang, C. et al. Prime-boost vaccination with chimpanzee adenovirus and modified vaccinia Ankara encoding TRAP provides partial protection against Plasmodium falciparum infection in Kenyan adults. *Sci. Transl. Med.* **7**, 286re285 (2015).
23. Folegatti, P. M. et al. Safety and immunogenicity of the ChAdOx1 nCoV-19 vaccine against SARS-CoV-2: a preliminary report of a phase 1/2, single-blind, randomised controlled trial.*Lancet* **396**, 467–478 (2020).
24. & Sadoff, J. et al. Interim results of a phase 1-2a trial of Ad26.COV2.S covid-19 vaccine.*N. Engl. J. Med.* **384**, 1824–1835 (2021).
25. Zhao, H. et al. Seroprevalence of neutralizing antibodies against human adenovirus type-5 and chimpanzee adenovirus type-68 in cancer patients. *Front Immunol.* **9**, 335 (2018).
26. Lundstrom, K. RNA viruses as tools in gene therapy and vaccine development. *Genes (Basel)* **10**, 189 (2019).
27. Mulligan, M. J. et al. Phase I/II study of COVID-19 RNA vaccine BNT162b1 in adults. *Nature* **586**, 589–593 (2020).
28. McNamara, M. A., Nair, S. K. & Holl, E. K. RNA-based vaccines in cancer immunotherapy. *J. Immunol. Res* **2015**, 794528 (2015).
29. Allen, T. M. et al. CD8+ Lymphocytes from simian immunodeficiency virus-infected rhesus macaques recognize 14 different epitopes bound by the major histocompatibility complex class i molecule Mamu-A*01: implications for vaccine design and testing. *J. Virol.* **75**, 738–749 (2001).
30. Bulik-Sullivan, B. et al. Deep learning using tumor HLA peptide mass spectrometry datasets improves neoantigen identification. *Nat. Biotechnol.*, https://doi.org/10.1038/nbt.4313 (2018).
31. Chen, E. X. et al. Effect of combined immune checkpoint inhibition vs best supportive care alone in patients with advanced colorectal cancer: the Canadian Cancer Trials Group CO.26 Study. *JAMA Oncol.* **6**, 831–838 (2020).
32. Bendell, J. et al. Efficacy and safety results from IMblaze370, a randomised phase III study comparing atezolizumab1cobimetinib and atezolizumab monotherapy vs regorafenib in chemotherapy-refractory metastatic colorectal cancer. *Ann. Oncol.* **29**, v123 (2018). 2018.
33. Grothey, A. et al. Fluoropyrimidine (FP) 1 bevacizumab (BEV) 1 atezolizumab vs FP/BEV in BRAFwt metastatic colorectal cancer (mCRC): findings from cohort 2 of MODUL–a multicentre, randomized trial of biomarkerdriven maintenance treatment following first-line induction therapy. *Ann. Oncol.* **29**, viii714–viii715 (2018).

34. Farber, D. L., Yudanin, N. A. & Restifo, N. P. Human memory T cells: generation, compartmentalization and homeostasis. *Nat. Rev. Immunol.* **14**, 24–35 (2014).
35. Trolle, T. et al. The length distribution of class I-restricted T cell epitopes is determined by both peptide supply and MHC allele-specific binding preference. *J. Immunol.* **196**, 1480–1487 (2016).
36. Wieczorek, M. et al. Major histocompatibility complex (MHC) class I and MHC class II proteins: conformational plasticity in antigen presentation. *Front Immunol.* **8**, 292 (2017).
37. Chudley, L. et al. Harmonisation of short-term in vitro culture for the expansion of antigen-specific CD8+ T cells with detection by ELISPOT and HLA-multimer staining. *Cancer Immunol. Immunother.* **63**, 1199–1211 (2014).
38. Zhang, Q. et al. Prognostic and predictive impact of circulating tumor DNA in patients with advanced cancers treated with immune checkpoint blockade. *Cancer Disco.* **10**, 1842–1853 (2020).
39. McGranahan, N. et al. Allele-specific HLA loss and immune escape in lung cancer evolution. *Cell* **171**, 1259–1271 (2017).
40. Rosenthal, R. et al. Neoantigen-directed immune escape in lung cancer evolution. *Nature* **567**, 479–485 (2019).
41. Paulson, K. G. et al. Acquired cancer resistance to combination immunotherapy from transcriptional loss of class I HLA. *Nat. Commun.* **9**, 3868 (2018).
42. Piperno-Neumann, S. et al. Phase 3 randomized trial comparing tebentafusp with investigator's choice in first line metastatic uveal melanoma.*Cancer Res.* **18**, CT002 (2021).
43. Rappaport, A. R. et al. Low-dose self-amplifying mRNA COVID-19 vaccine drives strong protective immunity in non-human primates against SARS-CoV-2 infection. *Nat. Commun.* **13**, 3289 (2022).

Methods

Ethics statement. The research presented in this paper complies with all the relevant ethical regulations. Animal studies were performed according to institutional animal care and use (IACUC)-approved protocol at the California National Primate Research Center at the University of California, Davis. The clinical study and all related analyses were carried out in accordance with the Declaration of Helsinki and Good Clinical Practice guidelines and was approved by the appropriate institutional review board (IRB) or ethics committees at each participating site (University of Chicago Comprehensive Cancer Center, Chicago, IL; Columbia University Medical Center, New York, NY; The Ohio State University Medical Center, Columbus, OH; Virginia Cancer Specialists, Fairfax, VA; Memorial Sloan Kettering Cancer Center, New York, NY; Peter MacCallum Cancer Centre, Melbourne, VIC, Australia; Mayo Clinic, Phoenix, AZ; Mayo Clinic, Rochester, MN; The University of Texas MD Anderson Cancer Center, Houston, TX). All patients provided written, informed consent. Further details can be found at https://clinicaltrials.gov/ct2/show/NCT03639714.

NHP study. *Animal selection and dosing.* Study was performed according to IACUC-approved protocol at the California National Primate Research Center at the University of California, Davis. Animals did not receive any prior treatment with immune-modulatory antibodies or vaccination against SIV and had no prior exposure to SIV. Animal groups and dosing are outlined in Supplementary Table 1. Briefly, both ChAd68 and samRNA were administered as bilateral i.m. injections into the quadriceps muscle. All ChAd68 doses were at 10^{12} VP with 2 ml total injection volume (1 ml per leg). All samRNA doses were at 300 µg with 1 ml total injection volume (500 µl per leg). Anti-CTLA-4 (ipilimumab) was administered as either an i.v. injection of 5 mg kg^{-1} or a flat dose of 50 mg per animal injected subcutaneously bilaterally near each vaccine site draining lymph node. Initial weights, doses of ipilimumab and treatment groups are shown below. Animals 37576 and 42300 were excluded from the study after week 20 with no further immune monitoring or immunizations due to recurrent issues with anemia and low-yield blood draws.

SIV model antigen cassettes. A model antigen cassette containing six previously published SIV viral epitopes[29] (SIV Gag CM9 (CTPYDINGQM), SIV Env TL9 (TVPWPNASL), SIV Env CL9 (CAPPGYALL), SIV Tat TL8 (TTPESANL), SIV Gag LW9 (LSPRTLNAW) and SIV Pol SV9 (SGPKTNIIV)) was designed. Each minimal epitope is embedded in a 25 amino acid sequence with 8 amino acids flanking each minimal epitope sequence. The cassette also contains class II helper epitopes. The cassette was synthesized by GenScript and designed to allow cloning into plasmids containing ChAd and samRNA vectors. The ChAd vector is an E1, E3 deleted virus, and the cassette expression was flanked by a cytomegalovirus promoter and an SV40 polyadenylation signal. The ChAd plasmid was digested with PacI and then transfected into HEK293 cells to generate virus. The virus for the NHP studies was made by CsCl gradient centrifugation and for the good manufacturing practice studies was purified by anion exchange chromatography. The same cassette was cloned into BstB1–PacI sites of a pBAC-VEE alphavirus-based plasmid that was used to make the samRNA RNA by in vitro transcription (TriLink) and then formulated into lipid nanoparticles (Arbutus).

Test articles (NHP study). Anti-CTLA-4 monoclonal antibody (mAb) (ipilimumab) was provided by Bristol Myers Squibb. ChAd68-MAG was generated by Gritstone Oncology (non-GLP) and prepared at 5×10^{11} VP ml^{-1} in Adenovirus Reference Material buffer (10 mM Tris, pH 8.0, 25 mM NaCl and 2.5% glycerol buffer). samRNA was generated by TriLink Biotechnologies and formulated in lipid nanoparticles by Arbutus.

Isolation of PBMCs and serum (NHP study). For immune monitoring, 10–20 ml blood was collected into vacutainer tubes containing heparin and maintained at room temperature until isolation. PBMCs were isolated by density centrifugation using lymphocyte separation medium and Leucosep separator tubes. PBMCs were counted using the Attune NxT (Thermo Fisher Scientific) and resuspended at a concentration of 4×10^6 cells ml^{-1} in complete RPMI.

IFN-γ ELISpot assay (NHP study). IFN-γ enzyme-linked immunospot (ELISpot) assays were performed using precoated 96-well plates (MAbtech, Monkey IFNγ ELISpot PLUS, ALP) following the manufacturer's protocol. Then, 10^5 PBMCs per well were plated in triplicate with 10 µg ml^{-1} peptide stimuli (GenScript) and incubated overnight in complete RPMI (RPMI + 10% FBS). A human hepatitis B virus S-antigen peptide not contained in the cassette (WLSLLVPFV, GenScript) was used as a negative control for each sample. Plates were washed with PBS and incubated with anti-monkey IFN-γ mAb biotin (MAbtech) for 2 h, followed by an additional wash and incubation with Streptavidin-ALP (MAbtech) for 1 h. After final wash, plates were incubated for ten minutes with BCIP/NBT (MAbtech) to develop the immunospots and dried overnight at 37°C. Spots were imaged and enumerated using AID reader (Autoimmun Diagnostika). For data processing and analysis, samples with replicate well variability (variability = variance/(median + 1)) greater than 10 and median greater than 10 were excluded[44]. Spot values were adjusted based on the well saturation according to the formula[45]:

$$\text{AdjustedSpots} = \text{RawSpots} + 2 * (\text{RawSpots} * \text{saturation}/(100 - \text{saturation})$$

Each sample was background corrected by subtracting the average value of the negative control peptide wells. Data are presented as SFU per 10^6 PBMCs. Wells with well saturation values greater than 50% were labeled as too numerous to count, and their value was set to the maximum measured SFU for that experiment.

ICS assay (NHP study). Freshly isolated PBMCs were distributed at 10^6 per well into V-bottom 96-well plates. Cells were pelleted and resuspended in 100 µl complete RPMI containing 1 µg ml^{-1} anti-CD28 mAb (CD28.2, BD Biosciences), 1 µg ml^{-1} anti-CD49d mAb (9F10, BD Biosciences) and 10 µg ml^{-1} pooled peptide antigens or human hepatitis B virus S-antigen peptide (WLSLLVPFV) as a negative control stimulant (GenScript). After 1 h of stimulation, Brefeldin A (Biolegend) was added to a final concentration of 5 µg ml^{-1} and incubated for an additional 16 h. Following stimulation, cells were washed with PBS and stained with fixable viability dye (eBioscience). Extracellular staining was performed in FACS buffer (PBS + 2% FBS + 2 mM EDTA) with anti-CD3, anti-CD4, anti-CTLA-4, anti-PD1 and anti-CD8 antibodies. Cells were washed, fixed and permeabilized with Transcription Factor fixation/permeabilization kit (eBioscience), and then intracellular staining was performed in permeabilization buffer. Samples were stained for IFN-γ, TNF-α, granzyme B and CD69. Samples were collected on the Attune NxT (Thermo Fisher Scientific). Gating strategy was as follows (Supplementary Fig. 1): lymphocytes (SSC-A versus FSC-A), single cells (SSC-H versus SSC-A), viable cells (SSC-A versus LD-506), $CD4^+$ or $CD8^+$ ($CD4^+$-phycoerythrin (PE) versus $CD8^+$-e450), cytokine$^+$ (TNF-α-BV421 versus IFN-γ-APC-R700).

Tetramer staining assay (NHP study). Following overnight rest at 4°C, isolated PBMCs were distributed into 96-well V-bottom plates at a density of 10^6 cells per 100 µl and stained with a viability dye (Live/Dead e506, eBioscience) in PBS for 20 min at 4°C. TCR recycling was inhibited by treatment with 50 nM Dasatinib for 1 h at 4°C. Cells were stained for 1 h at 4°C in FACS buffer with Mamu-A*01 tetramers for each of the peptide antigens with a unique combination of two fluorophores per antigen (produced in-house). Cells were co-stained for CD3 (A700, SP34.2, BD Biosciences), CD8 (e450, SK1, BD Biosciences), CD45RA (FITC, 5H9, BD Biosciences) and CCR7 (SB780, 3D12, eBioscience). Samples were collected on the Attune NxT (Thermo Fisher Scientific). The gating strategy was as follows (Supplementary Fig. 1): lymphocytes (SSC-A versus FSC-A), single cells (SSC-H versus SSC-A), viable cells (SSC-A versus LD-506), $CD3^+$ cells (SSC-A versus CD3-A700), $CD8^+$ (SSC-A versus CD8-e450), tetramer double positive (tetramer-UV405 versus tetramer-UV605; tetramer-UV405 versus tetramer-PE; tetramer-PE versus tetramer-UV675; tetramer-PE-Cy7 versus tetramer-UV405) and memory populations (CD45RA-FITC versus CCR7-SB780).

Cytotoxicity (T cell killing) assay (NHP study). Freshly isolated PBMCs for each sample were divided into two portions. T-cell enrichment was performed on one portion using the Miltenyi NHP T-cell isolation kit (130-092-143), following manufacturer's protocol and using MS columns (Miltenyi) to deplete non-T cells. The second portion (referred to as PBMCs) was stained with carboxyfluorescein succinimidyl ester (CFSE) at 1 mM (eBioscience). The CFSE-labeled PBMCs were then loaded with 50 mg ml^{-1} SIV peptides or a negative control peptide (WLSLLVPFV) by incubation for 1 h at 37°C in RPMI + 1% FBS. Isolated T cells and peptide-loaded target PBMCs were then counted and plated in a 20:1 ratio (T cells to target cells) in a V-bottom plate. Then, 400,000 T cells and 20,000 target cells were plated per well. Target cells only were also plated as a control. Cells were incubated for 6 h at 37°C in RPMI + 10% FBS. Following incubation, cells were stained with 7-AAD (Thermo Fisher Scientific) and immediately analyzed by flow cytometry using a Cytoflex LX (Beckman). $CFSE^+$ target cells were gated and 7-AAD^+ cells measured (as a percentage of $CFSE^+$ cells). Remnant T cells were also analyzed by flow cytometry to confirm T cell isolation. Samples were collected on the Attune NxT (Thermo Fisher Scientific). The gating strategy was as follows (Supplementary Fig. 1): lymphocytes (SSC-A versus FSC-A), single cells (SSC-H versus SSC-A), 7-AAD^+CFSE^+ (7-AAD versus CFSE).

Anti-ChAd68 neutralizing antibody assay (NHP and clinical study). Dilutions of heat-inactivated human and NHP sera were evaluated for the ability to neutralize a ChAd virus expressing the reporter protein beta-galactosidase (ChAd-LacZ). The reciprocal of the dilution that gives 50% or greater neutralization is used to assign a neutralization titer. In brief, pre- and post-vaccination serum samples were heat inactivated at 56°C for 30 min. Sera samples were then diluted twofold in serum-free media (DMEM) starting at 1:20 dilution down to 1:1,280. If needed, additional dilutions were made to get a titer within the range of the assay. The diluted samples were then mixed with an equal volume of media containing diluted virus sufficient to infect 293 A cells at an approximate multiplicity of infection (m.o.i.) of 1. The diluted sera and virus were incubated for 1 h at 37°C before adding onto 293 A cells plated at 2.5×10^4 cells/well on a 96-well tissue culture plate 1 day earlier. The cells and neutralizing mix were incubated for 1 h at 37°C and then an equal volume of media with 20% FBS was added. The cells and virus were then incubated for an additional 18–20 h before lysis and measurement of

B-galactosidase activity. Media was aspirated and the cells lysed in 100 µl lysis buffer from Thermo Fisher Scientific (Galacto-Star System). The cells were then freeze thawed twice (alternating −80 °C and 37 °C), mixed, and then 50 µl was mixed with an equal volume of Galacto-Star substrate (Thermo Fisher Scientific) for B-galactosidase measurement. Wells with media alone were used to determine expression in the absence of sera (100% B-galactosidase activity) and wells with no virus were used to determine the background of the assay. The percent inhibition was calculated for each dilution and plotted to generate a curve of percent neutralization versus dilution. A titer was assigned either as a limiting dilution titer, which is the reciprocal dilution that gives 50% or greater inhibition, or as interpolated from the dilution curve.

Phase 1 clinical trial. *Study design.* The study protocol is available in the Supplementary Information. The main objectives of this phase 1/2 study (NCT03639714) were to evaluate the safety and tolerability, immunogenicity and early clinical activity to determine and evaluate the RP2D of i.m. administration of GRT-C901 (ChAd68) and GRT-R902 (self-amplifying RNA formulated in lipid nanoparticles; samRNA), an individualized neoantigen cancer vaccine, in combination with i.v. nivolumab and s.c. ipilimumab, in patients with metastatic NSCLC, MSS-CRC, GEA and metastatic urothelial cancer. The phase 1 portion of the study was designed to find an RP2D using an adaptive dose-escalation method and modified toxicity probability interval-2 (mTPI-2) among the planned doses; DL1 through DL4 are outlined in Fig. 2a, with the goal of determining the highest vaccine dosage with a dose-limiting toxicity (DLT) rate below 30%.[46] All patients received 10^{12} VP ChAd68 prime and monthly i.v. anti-PD-1 antibody nivolumab administrations (480 mg every 4 weeks). Patients at DL1 and DL2 received 30 µg and 100 µg samRNA boosts, respectively. Patients at DL3 and DL4 received 100 µg and 300 µg samRNA, respectively, in addition to s.c. ipilimumab (30 mg) with each vaccination. ChAd68 boost was administered to eight patients with varying intervals at a dose of 10^{12} VP (Extended Data Table 1). The sample size was not driven by a statistical power due to the nature of an adaptive dose-escalation method. Therefore, the sample size of the phase 1 portion of the study ranged from 11 to maximum of 24 patients which is dependent on occurrence of DLTs. This study was carried out in accordance with the Declaration of Helsinki and Good Clinical Practice guidelines and was approved by the appropriate IRB or ethics committees at each participating site (University of Chicago Comprehensive Cancer Center, Chicago, IL; Columbia University Medical Center, New York, NY,; The Ohio State University Medical Center, Columbus, OH; and Virginia Cancer Specialists, Fairfax, VA). All patients provided written, informed consent. Further details can be found at https://clinicaltrials.gov/ct2/show/NCT03639714. Per protocol, patients had the potential to receive study treatment concurrent with ongoing standard-of-care chemotherapy.

The first patient enrolled on 24 September 2018 and the last patient enrolled on 25 November 2019 for the phase 1 portion of the study. As of the data cutoff date of 31 January 2022, a total of 29 patients (i.e., 14 patients in phase 1 and 13 patients in phase 2) have been treated, and the study is still ongoing to evaluate the efficacy of the RP2D using overall response rate, duration of response, clinical benefit rate, deepening of response, progression of survival and OS. Of the 14 phase 1 patients reported on in this study, patients G8, G9 and G10 received continued standard-of-care chemotherapy with study treatment. G8 received fluorouracil (5-FU) and bevacizumab (initiated 21 months before study treatment), and G9 and G10 received fluoropyrimidine/irinotecan (FOLFIRI) (initiated 12 and 8 months before study treatment). Four clinical sites enrolled and treated patients for the phase 1 part of the study: University of Chicago Comprehensive Cancer Center, Columbia University Medical Center, The Ohio State University Medical Center and Virginia Cancer Specialists. There is no data safety monitoring board for this study. A study committee consisting of the investigators and study sponsor meets regularly to assess the safety profile of the study treatment and make recommendations for dose escalation. Patient data were collected via electronic data capture and analyzed as described in the Statistics and reproducibility section.

Study population. *Inclusion criteria.* Inclusion criteria for vaccine production stage. Patients must meet the following inclusion criteria to be eligible for vaccine production stage:

1. Provide a signed and dated Informed Consent Form (ICF) document before initiation of study-specific procedures.
2. Patients with the indicated advanced or metastatic solid tumor as follows:
    a. NSCLC who are planned for or have received no more than one cycle of systemic treatment with cytotoxic, platinum-based chemotherapy (patients receiving anti-PD-(L)1 monotherapy are eligible)
    b. GEA who are planned for or have received no more than one cycle of systemic treatment with cytotoxic, platinum-based chemotherapy
    c. metastatic urothelial cancer who are planned for or have received no more than one cycle of systemic treatment with cytotoxic, platinum-based chemotherapy
    d. CRC-MSS who are receiving first-line systemic therapy or who are planned for or have received no more than one cycle of second-line systemic therapy including a fluoropyrimidine and oxaliplatin or irinotecan
3. Availability of formalin-fixed, paraffin-embedded (FFPE) tumor specimen for neoantigen assessment.
4. Measurable disease according to RECIST v1.1.
5. Lesions amenable to biopsy.
6. ≥12 years of age (patients 12–17 years of age must weigh >40 kg).
7. Life expectancy of > 6 months per the investigator.
8. ECOG performance status of 0 or 1 (or equivalent for patients 12–17 years of age based on Karnofsky or Lansky performance scale).
9. Patient has adequate organ function using values obtained within 4 weeks before starting routine therapy as defined below. The sponsor may consider patients eligible despite having a laboratory value that does not meet inclusion criteria provided the Investigator reports the patient is otherwise in good health and the history and kinetics of the change in the laboratory value do not raise a substantial safety concern over including the patient in the study or compromise the integrity of the study data. The sponsor and investigator must agree to include any patients with a laboratory value below the defined criteria below:
    a. Peripheral white blood cell (WBC) ≥3,000/mm^3
    b. Absolute lymphocyte count ≥800/mm^3
    c. Absolute neutrophils count (ANC) ≥ 1,500/mm^3
    d. Platelets ≥100,000/mm^3
    e. Hemoglobin ≥ 9 g dl^{-1}
    f. Albumin ≥ 3 g dl^{-1}
    g. Calculated creatinine clearance >50 ml min^{-1} using Cockcroft–Gault equation
    h. Alanine aminotransferase (ALT) and aspartate aminotransferase (AST) ≤3× upper limit of normal (ULN)
    i. Total bilirubin ≤1.5× ULN or direct bilirubin ≤1× ULN (patients with Gilbert's disease may be included if their total bilirubin is ≤3.0 mg dl^{-1})
    j. International normalized ratio or prothrombin time (PT) or partial thromboplastin time (PTT) ≤1.5× ULN
10. For NSCLC only, a history of smoking, defined as more than five packs, or 100 lifetime cigarettes.
11. For women of childbearing potential, willing to undergo pregnancy testing and agreeing to use at least one highly effective contraceptive method during the study treatment period and for 5 months after last investigational study treatment.

Inclusion criteria for study treatment stage. Patients must sign a second ICF and meet the following inclusion criteria to be eligible for the study treatment stage:

12. If patient did not participate in the vaccine production part of this study, patient has been enrolled in the screening protocol GO-003.
13. Provide a signed and dated ICF document before initiation of any treatment-related study-specific procedures.
14. Patient has received routine therapy as follows:
    i. Patient with NSCLC, metastatic urothelial cancer or GEA who has received systemic treatment with cytotoxic, platinum-based chemotherapy, has measurable disease according to RECIST v1.1 and:
        a. has chemotherapy and has an assessment of SD, partial response or complete response: will either receive study treatment in addition to continued routine therapy, or will receive study treatment after stopping routine therapy, per Investigator discretion; or
        b. has experienced disease progression: will receive study treatment as next line of therapy (i.e., without chemotherapy); or
        c. is intolerant to chemotherapy: will receive study treatment as next line of therapy (i.e. without chemotherapy)
    ii. Patient with CRC-MSS who has received second-line systemic therapy including a fluoropyrimidine and oxaliplatin or irinotecan, has measurable disease according to RECIST v1.1 and:
        a. has assessment of SD, partial response or complete response: will receive study treatment in addition to continued routine therapy per investigator discretion; or
        b. has experienced disease progression: will receive study treatment as next line of therapy; or
        c. is intolerant to chemotherapy: will receive study treatment as next line of therapy
15. Patient agrees to undergo research biopsies before study treatment and approximately 16 weeks after first vaccine administration (if patient has lesions amenable to biopsy).
16. ECOG performance status of 0 to 2 (or equivalent for patients 12–17 years of age based on Karnofsky or Lansky performance scale).
17. Patient has adequate organ function as defined below. The sponsor may consider patients eligible despite having a laboratory value that does not meet inclusion criteria provided the investigator reports the patient is otherwise in good health and the history and kinetics of the change in the laboratory value do not raise a substantial safety concern over including the patient in the study or compromise the integrity of the study data. The sponsor and

investigator must agree to include any patients with a laboratory value below the defined criteria below.

a. Peripheral WBC ≥2,000/mm^3
b. Absolute lymphocyte count ≥500/ mm^3
c. ANC ≥1,000/mm^3
d. Platelets ≥75,000/mm^3
e. Hemoglobin ≥ 9 g dl^{-1}
f. Calculated creatinine clearance >40 ml min^{-1} using Cockcroft–Gault equation
g. ALT and AST ≤3× ULN unless liver metastases are present in which case patients are included if ALT and AST ≤5 × ULN
h. Total bilirubin ≤1.5× ULN or direct bilirubin ≤1× ULN (patients with Gilbert's disease may be included if their total bilirubin is ≤ 3.0 mg dl^{-1}).
i. International normalized ratio and PT and PTT ≤1.5× ULN, unless patient is receiving anti-coagulant therapy, in which case patients are eligible if PT and PTT is within therapeutic range of intended use of anti-coagulants.

Exclusion criteria. *Exclusion criteria for the vaccine production stage.* Patients meeting any of the following criteria are not eligible for enrollment in the vaccine production stage:

1. Tumors with genetic characteristics as follows:
   a. For NSCLC, patients with a known genetic driver alteration in EGFR, ALK, ROS1, RET or TRK
   b. For CRC and GEA, patients with known microsatellite instability-high disease based on institutional standard
   c. For CRC, patients with a known BRAF V600E mutation or patients with peritoneal carcinomatosis, and for GEA, patients with peritoneal carcinomatosis as their only evidence of disease
2. Patient has a known tumor mutation burden more than one nonsynonymous mutations/megabase.
3. Known exposure to ChAd or any history of anaphylaxis in reaction to a vaccination or allergy or hypersensitivity to study drug components.
4. Bleeding disorder (e.g., factor deficiency or coagulopathy) or history of substantial bruising or bleeding following i.m. injections or blood draws.
5. Patient has received prior therapy consisting of anti-CTLA-4, anti-PD-1, anti-PD-L1 or any other antibody or drug specifically targeting T cell co-stimulation or checkpoint pathways.
   Patients with NSCLC and GEA who have been, or are currently being, treated with anti-PD-(L)1 monotherapy are eligible.
6. Immunosuppression that is expected to be present at the time of study treatment after vaccine production and coming from:
   a. Concurrent, recent (≤4 weeks) or anticipated treatment with systemic corticosteroids (>10 mg daily prednisone equivalent) or other immunosuppressive medications such as OKT3, ATG/ALG, methotrexate, tacrolimus, cyclosporine, azathioprine or rapamycin. Inhaled or topical steroids, physiologic corticosteroid replacement therapy for adrenal or pituitary insufficiency, steroid pretreatment for chemotherapy (e.g., pemetrexed), antihistamines, nonsteroidal anti-inflammatory drugs and aspirin are permitted in the absence of active autoimmune disease
   b. Conditions such as common variable hypogammaglobulinemia or radiation exposure such as large field radiotherapy
7. History of allogeneic tissue/solid organ transplant.
8. Patients who have had a history of life-threatening TRAEs with prior immunotherapy or have not recovered from prior cancer therapy-induced AEs (i.e., any AE that remains ≥ grade 2 or that has not returned to baseline with the exception of peripheral neuropathy, alopecia and hypothyroidism that is controlled with hormone replacement therapy).
9. Active, known or suspected autoimmune disease.
   a. Patients with type I diabetes mellitus, hypothyroidism, adrenal or pituitary insufficiency that is controlled with hormone replacement therapy, skin disorders (such as vitiligo, psoriasis or alopecia) not requiring systemic treatment, or conditions not expected to recur in the absence of an external trigger are permitted. Replacement therapy (e.g., thyroxine, insulin or physiologic corticosteroid replacement therapy for adrenal or pituitary insufficiency) is not considered a form of systemic treatment.
10. History of other cancer within 2 years with the exception of basal or squamous cell carcinoma of the skin, superficial bladder cancer or carcinoma in situ of the breast, cervix, prostate or other neoplasm that has undergone potentially curative therapy with no evidence of disease recurrence following agreement with sponsor.
11. Any severe concurrent non-cancer disease (including active systemic infection and/or uncontrolled hypertension) that, in the judgment of the investigator, would make the patient inappropriate for the current study.
12. Active tuberculosis or recent (<2 week) clinically substantial infection, or evidence of active hepatitis B or hepatitis C.
13. Known history of positive test for HIV or known acquired immunodeficiency syndrome.
14. History of pneumonitis requiring systemic steroids for treatment (with the exception of prior resolved in-field radiation pneumonitis).
15. Patient with known central nervous system (CNS) metastases and/or carcinomatous meningitis.
16. Myocardial infarction within 6 months of study initiation, active cardiac ischemia, myocarditis or New York Heart Association grade III or IV heart failure.
17. Pregnant, planning to become pregnant or nursing.
18. Medical, psychiatric, cognitive or other conditions that compromise the patient's ability to understand the patient information, give informed consent, comply with the study protocol or complete the study.

Exclusion criteria for the study treatment stage. Patients meeting any of the of the following exclusion criteria will not be eligible for the study treatment stage:

19. Immunosuppression from:
    - concurrent, recent (≤ 4 weeks) or anticipated treatment with systemic corticosteroids (>10 mg daily prednisone equivalent) or other immunosuppressive medications such as OKT3, ATG/ALG, methotrexate, tacrolimus, cyclosporine, azathioprine or rapamycin. Inhaled or topical steroids, physiologic corticosteroid replacement therapy for adrenal or pituitary insufficiency, steroid pretreatment for chemotherapy (e.g., pemetrexed), antihistamines, nonsteroidal anti-inflammatory drugs and aspirin are permitted in the absence of active autoimmune disease
    - conditions such as common variable hypogammaglobulinemia or exposures such as large field radiotherapy
20. Patients who have had history of life-threatening TRAEs with prior immunotherapy or who have not recovered from prior cancer therapy-induced AEs (i.e., any AE that remains ≥ grade 3, or that has not returned to baseline with the exception of alopecia, neuropathy and hypothyroidism if controlled by hormone replacement).
    Only applicable to those AEs not covered by other inclusion and exclusion criteria (e.g., ANC or ALT values).
21. Active, known or suspected autoimmune disease.
    Patients with type I diabetes mellitus, hypothyroidism if requiring hormone replacement, skin disorders (such as vitiligo, psoriasis or alopecia) not requiring systemic treatment, or conditions not expected to recur in the absence of an external trigger are permitted. Replacement therapy (e.g., thyroxine, insulin or physiologic corticosteroid replacement therapy for adrenal or pituitary insufficiency) is not considered a form of systemic treatment.
22. Received radiation therapy within 2 weeks before first dose of study treatment.
23. Any severe concurrent non-cancer disease (including active infection and/or uncontrolled hypertension) that, in the judgment of the investigator, would make the patient inappropriate for the current study (study treatment may be delayed until patient has recovered from disease (such as an infection) or has stabilized).
24. Active tuberculosis or recent (<2 week) clinically substantial infection, or evidence of active hepatitis B or hepatitis C.
25. History of pneumonitis requiring systemic steroids for treatment (with the exception of prior resolved in-field radiation pneumonitis).
26. Patient with uncontrolled CNS metastases or brain stem metastasis, patient receiving steroids for CNS disease and/or carcinomatous meningitis; patients with irradiated CNS metastases should be discussed on a case-by-case basis with the sponsor before enrollment.
27. Myocardial infarction, active cardiac ischemia, myocarditis or New York Heart Association grade III or IV heart failure since inclusion in the study.
28. Pregnant, planning to become pregnant or nursing.
29. Treatment with botanical preparations (e.g. herbal supplements or traditional Chinese medicines) intended for general health support or to treat the disease under study within 2 weeks before treatment that may interfere with study treatment per investigator discretion.
30. Medical, psychiatric, cognitive or other conditions that compromise the patient's ability to understand the patient information, give informed consent, comply with the study protocol or complete the study.

Individual patient-specific vaccine cassettes. Patient tissue next-generation sequencing, analysis and neoantigen prediction using the EDGE model were performed as previously described[30]. Twenty neoantigens were selected for each patient, as summarized in Supplementary Table 2. The 20 neoantigen epitopes were designed with flanking sequences so that each are 25 amino acids in length and arranged as a cassette to minimize generation of new junction epitopes. A class II helper domain consisting of universal class II epitopes PADRE and tetanus toxoid were included at the C terminus of the cassette. The cassettes were codon optimized for maximum protein expression in humans and for ease of synthesis. The cassettes were synthesized from overlapping oligonucleotides (Integrated

DNA Technologies (IDT)), that cover both DNA strands of the cassette sequence plus sequences in the plasmid backbones and assembled into either ChAd or samRNA plasmid backbones by Gibson assembly (Codex DNA). The assembled plasmids were then transformed into bacteria and screened by Sanger sequencing for correct clones which served as the templates for good manufacturing practice ChAd68 production or for samRNA transcription. ChAd68 plasmids were linearized with PacI and then transfected with TransIt Lenti (Mirus Bio) into 293F (Thermo Fisher Scientific) cells to initiate virus production. The virus was amplified through successive rounds of infection before the final production run at scale. The virus was purified at 48–72 h after infection and purified by anion exchange chromatography (Satorius) and formulated in 5 mM Tris, pH 7.9, 1 mM $MgCl_2$ and 75 mM NaCl. VP titers were determined by absorbance at 260 nm after SDS disruption and infectious unit titers were determined by immunostaining with an anti-Ad antibody (Abcam). samRNA plasmid was used as a template for RNA transcription using T7 polymerase, and the RNA was capped using a vaccine-capping enzyme and mRNA CAP 2′-*O*-methyl transferase (NEB). The RNA concentration was measured by Ribogreen quantitation and then formulated into lipid nanoparticles (Genevant).

Patient PBMC isolation and storage. Patient demographics and dosing schedules are shown in Table 1 and Extended Data Table 1. Due to COVID-19 restrictions, several blood draws were missed. Ad hoc dosing and blood draw timepoints were added with IRB approval for several patients. Whole blood for immunogenicity testing was collected before administration of the first dose (ChAd68 prime) to assess baseline levels and at 14 and 28 days (2 and 4 weeks) after ChAd68 prime. Subsequent planned sample collection post samRNA boosts include days 7, 14 and 28 after dose 2 (samRNA boost 1) and at days 7 and/or 28 after each additional samRNA boost. Two patients (G2 and G8) consented to an optional leukapheresis procedure (week 19 for G2, week 25 for G8). PBMCs from whole blood or leukopak were isolated at local PBMC processing sites according to standardized protocols. Briefly, cells were isolated using density gradient centrifugation on Ficoll Paque Plus (GE Healthcare), washed with D-PBS (Corning), counted and cryopreserved in CryoStor CS10 (STEMCELL Technologies) at 5×10^6 cells ml^{-1} for whole blood and 2×10^7 cells ml^{-1} for leukopak. Cryopreserved cells were stored in liquid N_2, shipped in cryoports and transferred to storage in liquid N_2 upon arrival. Cryopreserved cells were thawed and washed twice in OpTmizer T Cell Expansion Basal Medium (Gibco) with Benzonase (EMD Millipore) and once without Benzonase. Cell counts and viability were assessed using the Guava ViaCount reagents and module on the Guava EasyCyte HT cytometer (EMD Millipore). Cells were rested overnight before use in functional assays.

Peptides (clinical study). Custom-made, recombinant, lyophilized peptides specific for each patient were produced by GenScript and reconstituted at 5 mg ml^{-1} per peptide in sterile DMSO (VWR International), aliquoted and stored at −80 °C (Supplementary Table 2). Control peptides to assess responses to infectious disease antigens from cytomegalovirus, Epstein–Barr virus and influenza (CEF peptide pool) were purchased from JPT Peptide Technologies.

IVS cultures. Neoantigen-reactive T cells from patient samples were expanded in the presence of cognate peptides and low-dose IL-2 as described previously[30]. Briefly, thawed PBMCs were rested overnight and stimulated in the presence of minimal epitope peptide pools (10 µg ml^{-1} per peptide, 40 patient-specific peptides per pool) or control peptides (CEF) in ImmunoCult-XF T Cell Expansion Medium (IC media; STEMCELL Technologies) with 10 IU ml^{-1} recombinant human IL-2 (R&D Systems) for 14 days in 48- or 24-well tissue culture plates. Cells were seeded at 1-2 $\times 10^6$ cells/well and fed every 2–3 days by replacing two thirds of the culture media with recombinant human IL-2.

IFNγ ELISpot assay (clinical study). Detection of IFN-γ-producing T cells was performed by ex vivo ELISpot assay[47]. Briefly, cells were harvested, counted and resuspended in media at 4×10^6 cells ml^{-1} (ex vivo PBMCs) or 2×10^6 cells ml^{-1} (IVS-expanded cells) and cultured in the presence of DMSO (VWR International), phytohemagglutinin-L (Sigma-Aldrich), CEF peptide pool or cognate peptides in ELISpot Multiscreen plates (EMD Millipore) coated with anti-human IFN-γ capture antibody (Mabtech). Following 18–24 h incubation in a 5% CO_2, 37 °C, humidified incubator, supernatants were collected, cells were removed from the plate and membrane-bound IFNγ was detected using anti-human IFN-γ detection antibody (Mabtech), Vectastain Avidin peroxidase complex (Vector Labs) and AEC Substrate (BD Biosciences). ELISpot plates were allowed to dry, stored protected from light and sent to Zellnet Consulting for standardized evaluation[45]. Data are presented as SFU per million cells.

ICS (clinical study). PBMCs or IVS-expanded PBMCs were stimulated with either cognate minimal (8–11mer) or long overlapping (15mer) peptides, DMSO (vehicle control; VWR) or PMA/ionomycin cell stimulation cocktail (positive control; Affymetrix) in the presence of anti-human CD28/CD49d antibody (BD Biosciences), anti-human CD107α-BV421 (BioLegend), BD GolgiStop (BD Biosciences) and Brefeldin A (BioLegend) over a period of 18 h. Following overnight incubation, cells were stained with live/dead ZombieRed (BioLegend) and surface marker antibodies (CD8-PerCP-Cy5.5, CD3-BV605, CCR7-PE-Cy7 from BioLegend; CD4-APC-eF780, CD45RA-SuperBright702 from eBioscience; PD-1-BUV737 from BD Biosciences) before fixation and permeabilization with FIX & PERM Cell Permeabilization Kit (Thermo Fisher Scientific). Following permeabilization, cells were stained for intracellular cytokines using anti-human IFN-γ-APC, TNF-α-BV785, and IL-2-PE antibodies (BioLegend) before data acquisition on a BD LSRFortessa flow cytometer (BD Biosciences).

HLA class I fluorophore-conjugated tetramer generation and staining (clinical study). HLA class I tetramers were generated from Flex-T biotinylated HLA monomers (BioLegend) or MBL International with target peptides loaded onto the monomers by UV exchange according to the manufacturer's instructions. Successful loading of target peptides by UV exchange was assessed by ELISA (BioLegend, according to manufacturer's instructions). Alternatively, biotinylated monomers were generated in-house and prefolded with target peptides. pHLA monomers were assembled into tetramers using fluorophore-conjugated Streptavidin (PE from BioLegend; APC from eBioscience). Using generated fluorophore-labeled peptide-MHC tetramers, PBMCs were tetramer stained to help identify antigen-specific T cells. Patient PBMC samples were thawed and resuspended in a 96-well V-bottom plate with FACS buffer (PBS, 10% FBS [v/v]). Before staining, samples were incubated with 50 nM Dasatinib (Sigma-Aldrich) in a 5% CO_2, 37 °C incubator for 30 min. Subsequently, HLA class I fluorophore-labeled tetramers loaded with target peptides of interest were added directly to each corresponding PBMC sample. In instances where multiple tetramers needed to be added to the same sample, a cocktail was made with equal amounts of each tetramer, then mixed and added at the same time. Samples were incubated at room temperature for 1 h in the dark. Following incubation, samples were washed in FACS buffer and stained with an antibody master mix containing purified anti-human HLA-A,B,C antibody, anti-human CD8-PerCP-Cy5.5, anti-human CCR7-PE-Cy7, anti-human CD3-BV421 (all BioLegend), anti-human CD45RA-SB702, anti-human CD4-APC-eF780 (both eBioscience) and Live/Dead Green (Thermo Fisher Scientific). Sample were mixed and incubated at 4 °C in the dark protected from light for 20 min. Samples were washed once with FACS buffer and then resuspended in FACS buffer prior to acquisition on a BD LSRFortessa flow cytometer (BD Biosciences).

Flow cytometry analyses (clinical study). Samples acquired on flow cytometers were analyzed using FlowJo software (FlowJo). Gating strategies for human samples are as follows (Supplementary Figs 2 and 3). For CD4 versus CD8 T cell assessments: lymphocytes (SSC-A versus FSC-A), single cells (FSC-H versus FSC-A), viable cells (FSC-A versus LD-ZombieRed), $CD3^+$ cells (FSC-A versus CD3-BV605), $CD4^+$ and $CD8^+$ (CD4-APCeF780 versus CD8-PerCP-Cy5.5). For tetramer studies: lymphocytes (SSC-A versus FSC-A), single cells (FSC-H versus FSC-A), viable cells (FSC-A versus LD-AF488), $CD3^+$ cells (FSC-A versus CD3-BV421), $CD8^+Tet^+$ (CD8-PerCP-Cy5.5 versus tetramer-PE or tetramer-APC), memory phenotypes (CD45RA-SB702 versus CCR7-PE-Cy7). For ICS studies: lymphocytes (SSC-A versus FSC-A), single cells (FSC-H versus FSC-A), viable cells (FSC-A versus LD-ZombieRed), $CD3^+$ cells (FSC-A versus CD3-BV605), $CD4^+$ and $CD8^+$ (CD4-APCeF780 versus CD8-PerCP-Cy5.5), $CD8^+$ or $CD4^+$ $cytokine^+$ cells (CD8-PerCP-Cy5.5 versus CD107a-BV421, IFN-γ-APC, TNF-α-BV786, IL-2-PE; CD4-APCeF780 versus CD107a-BV421, IFN-γ-APC, TNF-α-BV786, IL-2-PE). Polyfunctionality analyses were performed using Boolean gating (FlowJo) and graphed using SPICE software v6 (ref. [48]). Results are represented as the percentage of positive cell populations (frequency of parent). Data are shown as background subtracted where indicated.

MSD U-plex assay. Detection of secreted IL-2, TNF-α and granzyme B (GRZB) in ex vivo ELISpot supernatants was performed using a U-plex assay MSD U-PLEX Biomarker assay. Assays were performed according to the manufacturer's instructions. Data were acquired on the MESO SECTOR S 600 instrument and DISCOVERY WORKBENCH assay analysis software. Analyte concentrations (pg ml^{-1}) were calculated using serial dilutions of known standards for each cytokine. For graphical data representation, values below the minimum range of the standard curve were represented as zero.

Triplex FluoroSpot assay. A multiplexed FluoroSpot assay was performed according to manufacturer's instructions (MABtech) on a subset of patient samples for the detection of IFN-γ, IL-2 and granzyme B-producing T cells. Briefly, patient PBMCs were thawed and rested overnight at 2×10^6 cells ml^{-1}. The following day, cells were harvested, counted and resuspended at 4×10^6 cells ml^{-1} before plating. Precoated FluoroSpot plates were washed with PBS and blocked with culture media before patient-specific peptide pools and cells were added (2×10^5 PBMCs per well). After incubating in a 5% CO_2, 37 °C humidified incubator for 18–24 h, secreted IFN-γ, IL-2 and granzyme B were detected using anti-human IFN-γ-BAM/anti-BAM-490, biotinylated anti-human granzyme B/Streptavidin-550 and anti-human-IL-2-WASP/anti-WASP-650 antibody pairs followed by fluorescence enhancer. Plates were imaged and enumerated on an AID iSpot reader (Autoimmun Diagnostika). Data are presented as SFU per million cells.

Single-cell TCR sequencing and digital gene expression. Single-cell library preparation and sequencing was completed according to 10x Genomics v1 5' Chromium Single Cell V(D)J protocol CG000186 Rev A. The only deviation in library preparation was in V(D)J library step 5.4 with five cycles of PCR. All sequencing was completed on the Illumina NovaSeq at a loading concentration of 450 pM with 5% PhiX. The 10x Genomics Cell Ranger version 3.1 was used for V(D)J and Digital Gene Expression library analysis and was current at time of research.

Adaptive TCR sequencing of RNA later-preserved tumor samples. Tumor DNA was extracted via Qiagen AllPrep DNA/RNA kit and quantified with both Qubit high sensitivity dsDNA assay (Thermo Fisher Scientific) and Agilent Genomic DNA tape on the 4200 TapeStation system. Between 300 and 1,000 ng extracted DNA was sent to Adaptive Biotechnologies for T cell receptor beta sequencing, and results were returned to us via the immunoSEQ Analyzer 3.0.

TCR sequencing analysis. Significant tumor TCR expansion was determined via a binomial test with Benjamini–Hochberg correction and P value <0.05, analyzing TCRs with five cells or more in either timepoint. IVS TCR expansion was analyzed by filtering 10× V(D)J results for each timepoint for TCRs (1) with a full alpha/beta pair, (2) found above an abundance threshold and (3) not found in the CEF IVS. The proportion of the resulting TCRs was then tracked from baseline to on treatment, and the polyfunctional activation of these expanded TCR populations was also analyzed by searching in the transcriptome for non-zero expression of IFN-γ, granzyme B, TNF and IL-2. The expanded TCRs were cross-referenced with those expanded in the tumor biopsies, and overlap was statistically significant by Fisher test ($P < 0.001$).

cfDNA collection and isolation. Whole blood was collected in two 10-ml cell-free DNA (cfDNA) BCT (Streck) starting at the time of the prime, and subsequent draws were collected at dosing visits. Due to COVID-19 restrictions, several blood draws were missed. Whole blood underwent a double-spin protocol to first separate plasma from WBCs and red blood cells before a second spin to remove any remaining cellular debris. The separated plasma was frozen and shipped to Gritstone Bio and stored at −80°C until extraction. cfDNA was extracted from the entire plasma volume of a single draw using the Apostle MiniMax cfDNA Isolation kit (ApostleBio) and quantified using the Qubit 1x dsDNA High Sensitivity Assay (Thermo Fisher Scientific).

ctDNA sequencing and analysis. Custom hybrid capture panels were designed for each patient enrolled in the study. Each patient panel was designed to capture the EDGE-predicted neoantigens and all predicted coding (nonsynonymous) mutations present in the original screening biopsy specimen. Target mutations for each patient were curated and sent for customized design to IDT as xGen Lockdown Probes. Each capture pool contained up to nine patients per pool. Patient-matched genomic DNA was fragmented before library preparation using the NEB FS module (NEB). Shotgun libraries for cfDNA (up to 30 ng) and the fragmented, patient-matched genomic DNA (20–30 ng) were prepared using the KAPA HyperPrep (KAPA Biosystems) kit using a customized pool of duplex adapters containing unique molecular identifiers for duplex sequencing (IDT). Shotgun libraries were captured with patient-specific probes overnight using the IDT xGen Hybridization and Wash kit. Enriched libraries were sequenced on an Illumina NovaSeq to a minimum mean raw depth of 80,000×. Briefly, unique molecular identifiers were clipped from the raw sequencing reads before alignment to hg38 using BWA-MEM. Using fgbio, aligned reads were grouped by position and duplex identity. Consensus reads were created using a duplex of 3× (three supporting reads from each strand) and realigned to hg38. Variant calling was performed using FreeBayes and filtered for the patient-specific variants. Variant allele frequency was converted to mutated haploid genomic equivalents per milliliter plasma (hGE ml^{-1}) using the extracted plasma volume and total cfDNA yield from the extraction. Percent change in ctDNA was calculated as the change of the median mutated hGE ml^{-1} from the baseline sample.

Patient tumor biopsy whole-exome and transcriptome analysis and TCGA data comparison. Pretreatment GRANITE patient FFPE biopsy-derived DNA and RNA and matched whole blood-derived DNA were whole-exome sequenced (IDT xGen V1) and analyzed as described previously[38]. Relevant tumor types for genomic comparison from TCGA Pan-Cancer Atlas dataset included gastric ($n = 405$ stomach adenocarcinoma), colon adenocarcinoma ($n = 332$, MSS-CRC (281) and MSI-CRC (51)), lung adenocarcinoma ($n = 498$), lung squamous cell carcinoma ($n = 463$, LUSC) and melanoma ($n = 436$, skin cutaneous melanoma). For RNA expression analyses, all GRANITE and TCGA sample RNA-seq by Expectation-Maximization expected counts were normalized utilizing DESeq2 (ref. [49]). Normalized counts were used to determine patient PD-L1 RNA expression and the IFN-γ RNA expression signatures, which were calculated as the average of 28 IFN-γ-associated gene specific z-scores across all GRANITE and TCGA samples ($n = 2,494$)[50]. Tumor mutational burden was calculated for each GRANITE patient as the total of all somatic variants called >4% variant allele frequency divided by the exome bait panel size (39 Mb). For TCGA samples, total mutations called were divided by exome bait panel size used (38 Mb)[51] (Supplementary Table 4).

Transduction, culture and live sorting of single HLA-expressing A375 NucLight Red cell lines. A375 cells were obtained from ATCC (CRL-1619). Endogenous class I HLAs were knocked out using CRISPR-Cas9 ribonucleoprotein complexes. HiFi S.p. Cas9 Nuclease V3 (1081060), Cas9 Electroporation Enhancer (1075915) and custom guide RNAs were obtained from IDT. Ribonucleoproteins were electroporated into A375 cells using the Neon transfection system from Thermo Fisher Scientific with a voltage of 1,400 and two pulses for 20 ms. CRISPR-treated A375 cells were stained using a 1:100 anti-human HLA-A,B,C antibody from Biolegend (311405), and HLA-null cells were sorted using the Cell Sorter SH800S (SONY Biotechnology) (Supplementary Fig. 4). Single-allele A375 cell lines were generated with HLA sequences obtained from the coding sequence of the human genome (HLA-B*08:01:01:01, HLA-B*57:01:01:01, HLA-A*30:04:01:01, HLA-A*03:01:01:01, HLA-C*04:01:01:01). HLAs were cloned into the pCDH-EF1α-MCS1 lentiviral expression backbone vector from System Biosciences (CD502A-1). Lentivirus was generated for each HLA and titer determined using the Lenti-X qRT-PCR titration kit from Takara Bio (631235). Single HLAs were transduced into A375 HLA-null cells at an m.o.i. of 100 with 8 ug ml^{-1} polybrene (EMD Millipore, TR-1003). Cells were spinoculated at 800g for 45 min at room temperature at a density of 8×10^5 cells per ml. Fresh media was added and cells were incubated overnight. HLA-positive cells were sorted after at least 48 h using the method described above. Fluorescent single-allele A375 cells were generated with NucLight Red (IncuCyte, 4476) at an m.o.i. of 3 with 8 μg ml^{-1} polybrene (EMD Millipore, TR-1003). Cells were spinoculated at 800g for 45 min at room temperature at a density of 8e5 cells ml^{-1}. Fresh media was added and cells were incubated overnight. Red fluorescent and HLA-positive cells were sorted after at least 48 h using the method described above.

IncuCyte killing assays. Single HLA-expressing A375 NucLight Red cell lines were seeded in 96- or 48-well plates at concentrations of 2.5×10^4 or 3.5×10^4 cells per well in DMEM with 10% heat-inactivated FBS. The plates were placed in the IncuCyte S3 (Essen Biosciences) and 24 h after the seeding, the effector cells were plated at a concentration of 2.5×10^5 or 3.5×10^5 cells per well in a 96- or 48-well plate, respectively, for an effector to target ratio of 10:1. Individual peptides (GenScript; Supplementary Table 2) were added to the treated wells for a final concentration of 10 μg ml^{-1}, and DMSO was used for the control wells. The plates were imaged with the IncuCyte for up to 72 h, after which the data were analyzed using the IncuCyte S3 2018 analysis software. Viability of A375 was assessed by red cell count, and relative viability was calculated relative to DMSO co-culture control wells.

Statistics and reproducibility. For the clinical study, the sample size is not driven by a statistical power due to the nature of an adaptive dose-escalation method. Therefore, the sample size of the phase 1 portion of the study ranges from 11 to maximum of 24 patients, which is dependent on occurrence of DLTs. No data were excluded from the analyses, and experiments were not randomized. The investigators were not blinded to allocation during experiments and outcome assessment. For the NHP study, the number of animals per group is $n = 3$/sex, which is the minimum number of animals needed to do simple statistics. The total number of animals used in this study is considered the minimum required to properly characterize the effect of the test articles (i.e., vaccine and anti-CTLA-4) and compare their route of administration (i.e., s.c. versus i.v.) and has been designed such that it does not require an unnecessary number of animals to accomplish its objectives. For both the NHP and clinical study, descriptive statistics are described throughout. Where applicable, statistical analyses applied for specific methods are outlined in the relevant methods sections.

Reporting summary. Further information on research design is available in the Nature Research Reporting Summary linked to this article.

Data availability

Deidentified individual participant clinical data that underlie the results reported in this article are available for transfer. Interested investigators can obtain and certify the data transfer agreement and submit requests to the principal investigator (K.J.). Investigators and institutions who consent to the terms of the data transfer agreement form, including, but not limited to, the use of these data for the purpose of a specific project and only for research purposes, and to protect the confidentiality of the data and limit the possibility of identification of participants in any way whatsoever for the duration of the agreement, will be granted access. Gritstone bio will then facilitate the transfer of the requested deidentified data. This mechanism is expected to be via a Gritstone Secure File Transfer Service, but Gritstone bio reserves the right to change the specific transfer method at any time, provided appropriate levels of access authorization and control can be maintained. Source data are provided with this paper. Pan-Cancer Atlas data sets were obtained from the cBioPortal (https://www.cbioportal.org/) and the UCSC Xena TCGA Pan-Cancer Atlas data hub (https://pancanatlas.xenahubs.net), and raw data are available through the Genomic Data Commons (https://gdc.cancer.gov/). Epitope selection and patient-specific neoantigen selection used a previously published algorithm[30]. Source data are provided with this paper.

References

44. Moodie, Z. et al. Response definition criteria for ELISPOT assays revisited. *Cancer Immunol. Immunother.* **59**, 1489–1501 (2010).
45. Janetzki, S. et al. Guidelines for the automated evaluation of Elispot assays. *Nat. Protoc.* **10**, 1098–1115 (2015).
46. Ji, Y. & Wang, S. J. Modified toxicity probability interval design: a safer and more reliable method than the 3+3 design for practical phase I trials. *J. Clin. Oncol.* **31**, 1785–1791 (2013).
47. Janetzki, S., Cox, J. H., Oden, N. & Ferrari, G. Standardization and validation issues of the ELISPOT assay. *Methods Mol. Biol.* **302**, 51–86 (2005).
48. Roederer, M., Nozzi, J. L. & Nason, M. C. SPICE: exploration and analysis of post-cytometric complex multivariate datasets. *Cytom. A* **79**, 167–174 (2011).
49. Love, M. I., Huber, W. & Anders, S. Moderated estimation of fold change and dispersion for RNA-seq data with DESeq2. *Genome Biol.* **15**, 550 (2014).
50. Ayers, M. et al. IFN-γ-related mRNA profile predicts clinical response to PD-1 blockade. *J. Clin. Invest.* **127**, 2930–2940 (2017).
51. Chalmers, Z. R. et al. Analysis of 100,000 human cancer genomes reveals the landscape of tumor mutational burden. *Genome Med* **9**, 34 (2017).

Acknowledgements

We would like to thank the patients and their families; clinical staff and study coordinators; Bristol Myers Squibb for providing ipilimumab and nivolumab; and K. Caldwell, A. Dixon, C. Voong, J. Abhyankar, G. Talbot, A. Bezawada, W. Zhai, M. Zhong, T. Patch and J. Rouhana. We also thank T. Chan for critical review and guidance. Funding was provided by the study sponsor, Gritstone bio. Employees of Gritstone bio received salaries for study conceptualization, design, data analyses, decision to publish and manuscript preparation. No other authors received specific funding for this work from the sponsor.

Author contributions

C.D.P., A.R.R., M.D., M.S., G.G., W.B., R.R., R.Y., A.A., A.F. and K.J. designed the study and wrote the manuscript. C.D.P., A.R.R., M.D., M.G.H., C.D.S., L.D.K., S.K., A.Y., L.S., D.S., M.S., K.T., M.M., J.R.J., C.N.N., E.M., R.Z., D.N.G., A.C.G., R.G., K.B., M.D.C. and R.Y. contributed to experimental design, execution and data analysis. A.I.S., S.R., D.C., B.S.H., C.G.D., B.J.S., D.A., A.M., S.B.M., B.J., R.R., C.-Y.L., D.V.T.C. and A.R.F. contributed to clinical oversight, patient recruitment, enrollment and treatment. C.D.S., L.G., S.-J.H., W.B., M.D.C., S.C. and K.J. contributed to vaccine design and production.

Competing interests

C.D.P., A.R.R., M.G.H., C.D.S., L.G., S-.J.H., L.D.K., S.K., D.S., M.D., M.M., J.R.J., C.N.N., R.Z., D.N.G., A.C.G., M.D.C., S.C., K.B., R.R., A.A., A.R.F., K.J., A.Y., L.S., M.S., K.T., E.M., G.G., R.G., W.B. and R.Y. are stockholders and either current or previous employees at Gritstone bio and may be listed as co-inventors on various pending patent applications related to the vaccine platform presented in this study. D.V.T.C. consults/has consulted/has advisory/had advisory roles at Genentech/Roche, Eli Lilly, Merck, Daiichi Sankyo, BMS, Ono, Five Prime, Seattle Genetics, Amgen, Taiho, Astellas, Gritstone bio, Pieris, Zymeworks, Basilea, QED, Foundation Medicine, Pierian, Silverback Therapeutics, Servier, Blueprint Medicines, Arcus Biosciences, Tempus, Guardant Health, Archer and Natera. C.G.D. is currently employed by Janssen R&D. B.S.H. has/had consultant/advisory roles for AstraZeneca, Ideaya, Jazz Pharmaceuticals, and research support from Neximmune. B.J.S. consults/has consulted/had advisory roles for Bristol Myers Squibb, Merck Sharp & Dohme, AstraZeneca, Pfizer, Roche/Genentech, Amgen, Lilly, Sanofi-Regeneron, Glaxo-Smith Kline, Takeda, Novartis and Beigene; has received honoria from Bristol Myers Squibb, Merck Sharp & Dohme, AstraZeneca, Pfizer, Roche/Genentech, Amgen, Lilly, Sanofi-Regeneron, Glaxo-Smith Kline, Takeda, Novartis and Beigene; has received research funding from Sanofi-Regeneron; and has received royalties from UpToDate. B.J. consulted for/had advisory roles with Taiho Oncology, Insmed Oncology, Gritstone bio, Pfizer and Incyte and received research funding from Gateway for Cancer Research, Bristol Myers Squibb and Syntrix. A.M. is on the Advisory Board for AstraZeneca, QED, and Taiho Oncology. S.R. participated in Advisory Boards for Incyte Corporation (2017), AbbVie (2017), QED Therapeutics (2018, 2019) and Bayer (2020) (healthcare companies <10,000 USD). S.R. received honoraria from IDT (2017) and Illumina (2018) (technology companies). S.R. received consulting fees from QED Therapeutics (2018, 2019) and Merck (2019) (healthcare companies <10,000 USD). S.R. received travel reimbursement from Incyte Corporation (2019) (<999 USD). C.Y.L. received honoraria from Cancer Experts Now and has consulting/advisory board roles with Transthera, BluePrints Medicine, Genentech, QED Therapeutics, Histosonics and Ipsen and is part of the Speaker's Bureau for Eisai and Incyte. S.B.M. received honoraria from Natera, Bicara, Novartis, Basilea and Daiichi Sankyo and owned stock in Calithera outside the submitted work. The remaining authors declare no competing interests.

Additional information

Extended data is available for this paper at https://doi.org/10.1038/s41591-022-01937-6.

Supplementary information The online version contains supplementary material available at https://doi.org/10.1038/s41591-022-01937-6.

Correspondence and requests for materials should be addressed to Karin Jooss.

Peer review information *Nature Medicine* thanks Robert Seder and the other, anonymous, reviewer(s) for their contribution to the peer review of this work. Primary Handling editors: Saheli Sadanand and Joao Monteiro, in collaboration with the Nature Medicine team.

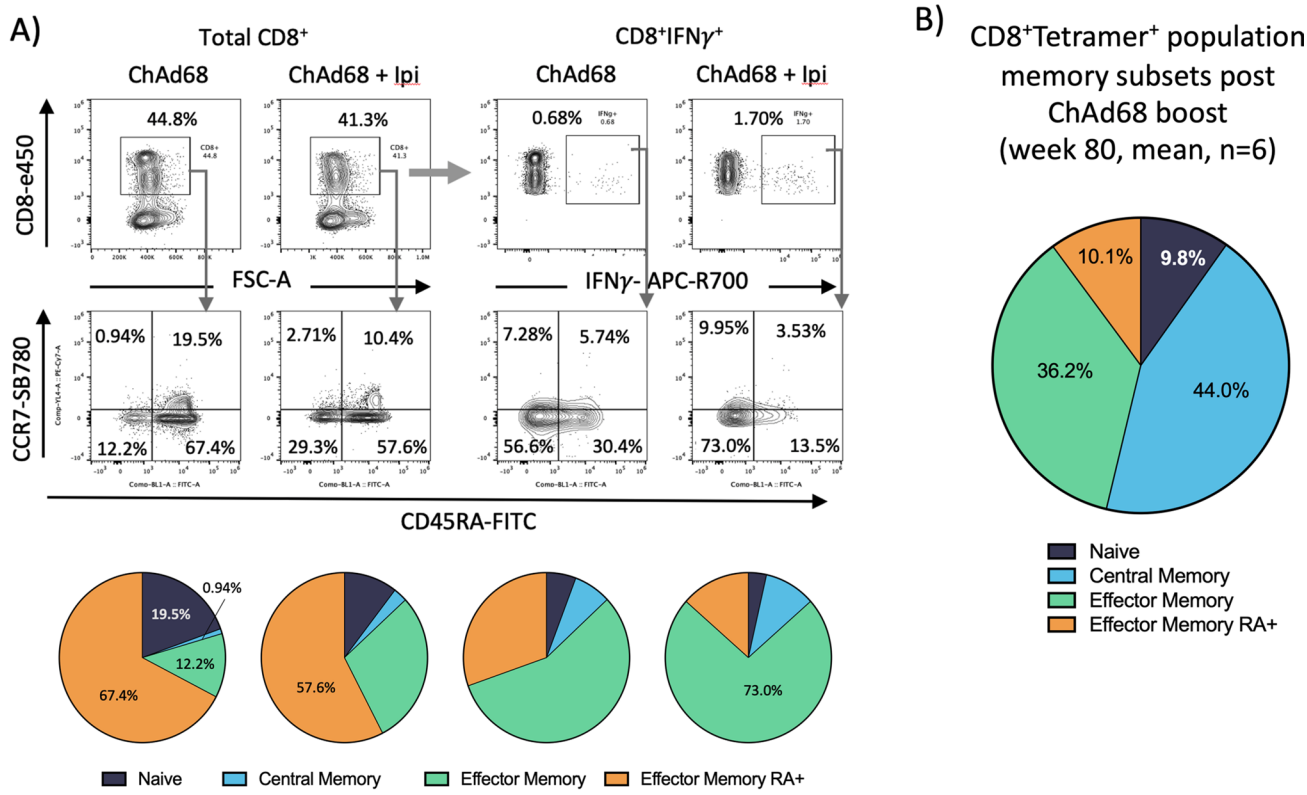

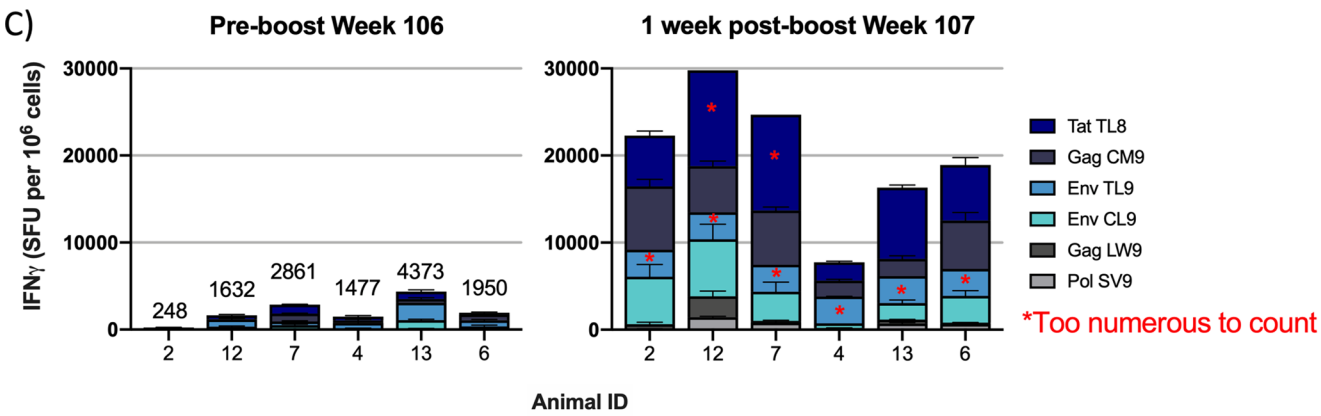

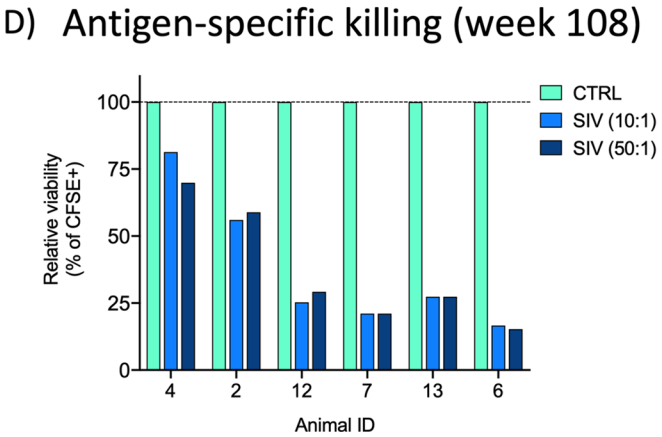

Extended Data Fig. 1 | See next page for caption.

Extended Data Fig. 1 | (**A)** Representative FACS plots (NHP 4 and NHP 10) and pie charts for each population (% of total $CD8^+$ or % of $CD8^+IFN\gamma^+$, mean for each group (n = 6 per group), week 13 post prime (one week post samRNA boost). Analysis of antigen-specific ($IFN\gamma^+$) memory T cell populations, using CCR7 and CD45RA (Naïve: $CCR7^+CD45RA^+$, purple; Central Memory: $CCR7^+CD45RA^-$, blue, Effector memory: $CCR7^-CD45RA^-$, green; Effector memory RA^+: $CCR7^+CD45RA^+$, orange). Pie chart represents mean percent of total tetramer population. (**B)** Analysis of memory T cell populations at 80 weeks post prime (1 year post last boost). Antigen-specific T cells were identified by combinatorial tetramer staining for six different antigens. Memory analysis was performed on total tetramer+ population, using CCR7 and CD45RA (Naïve: $CCR7^+CD45RA^+$, purple; Central Memory: $CCR7^+CD45RA^-$, blue, Effector memory: $CCR7^-CD45RA^-$, green; Effector memory RA^+: $CCR7^+CD45RA^+$, orange). Pie chart represents mean percent of total tetramer population (n = 6). (**C)** Antigen-specific T cell response in each individual animal (n=6 animals) 2 years post prime (week 106) and one week post samRNA boost (week 107), for six SIV antigens, as measured by IFNγ ELISpot. SFU/10^6 to each antigen (mean of three technical replicates per antigen with SD; negative control value subtracted) stacked to provide sum total response. Red asterisk represents values that were too numerous to count and were set to maximum measured value (11000 for TL8, plated at $2.5x10^4$ cells/well, and 3100 for TL9, plated at $1x10^5$ cells/well). (**D)** Killing of antigen loaded target cells by CD8 T cells (collected 2 weeks post-boost, week 108), relative viability of SIV-loaded PBMCs (as determined by 7-AAD staining), normalized to negative control peptide-loaded PBMCs for each sample, at specified effector to target ratios.

A)

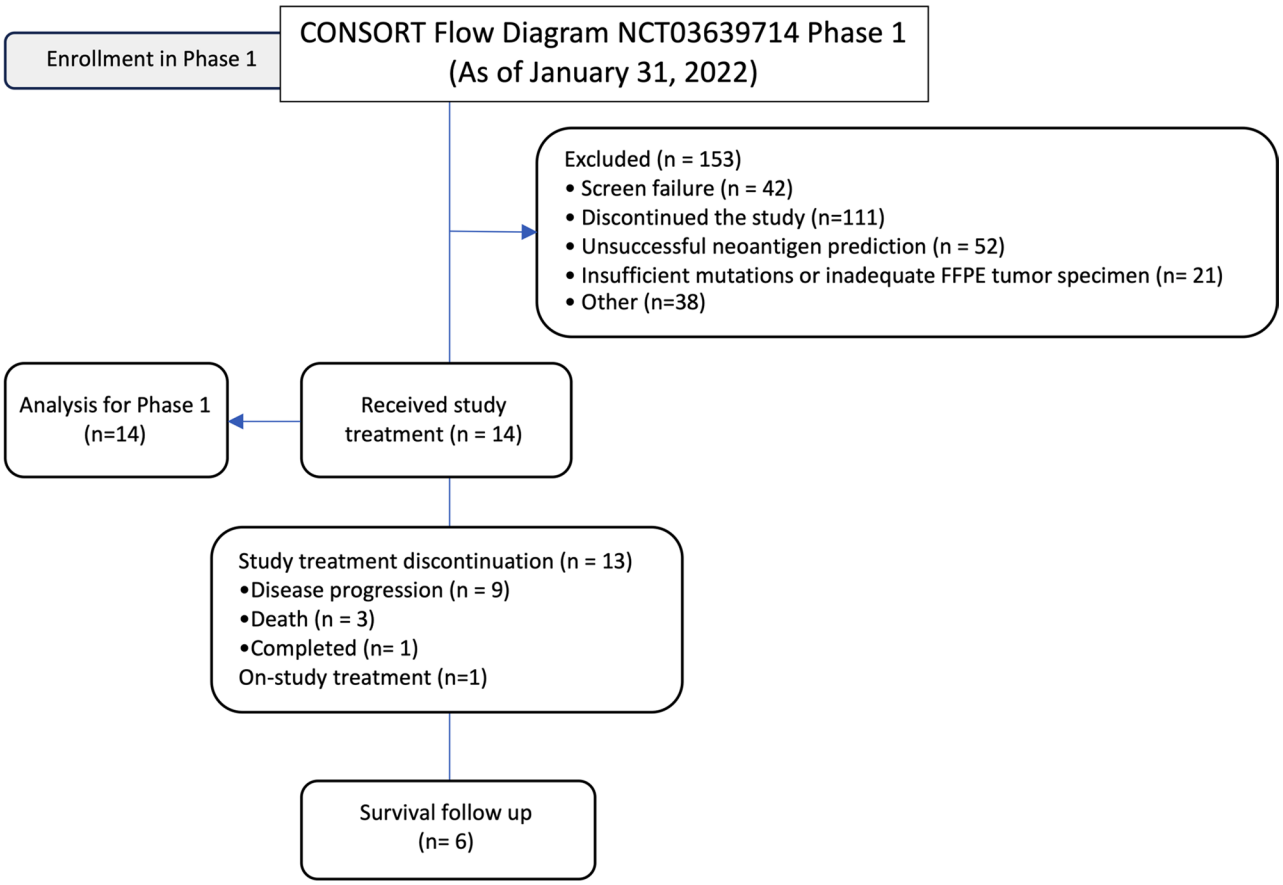

B)

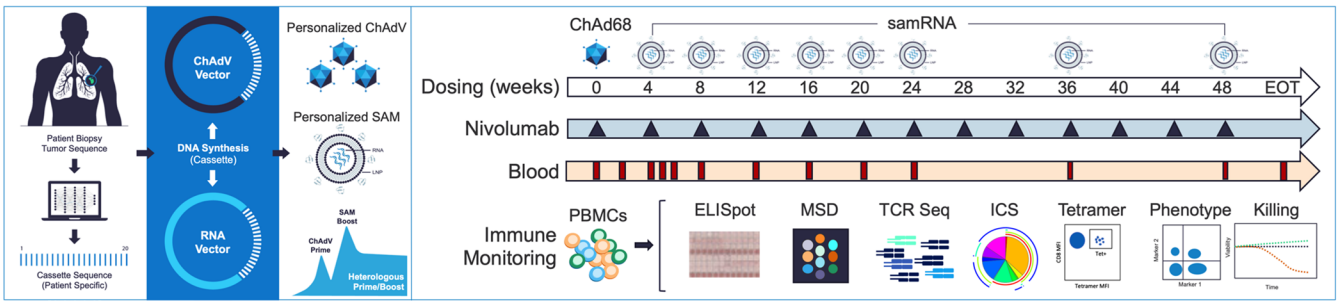

Extended Data Fig. 2 | (**A**) CONSORT flow diagram of patient enrollment. (**B**) Schematic outlining personalized vaccine production, planned dosing schedule, and immune monitoring.

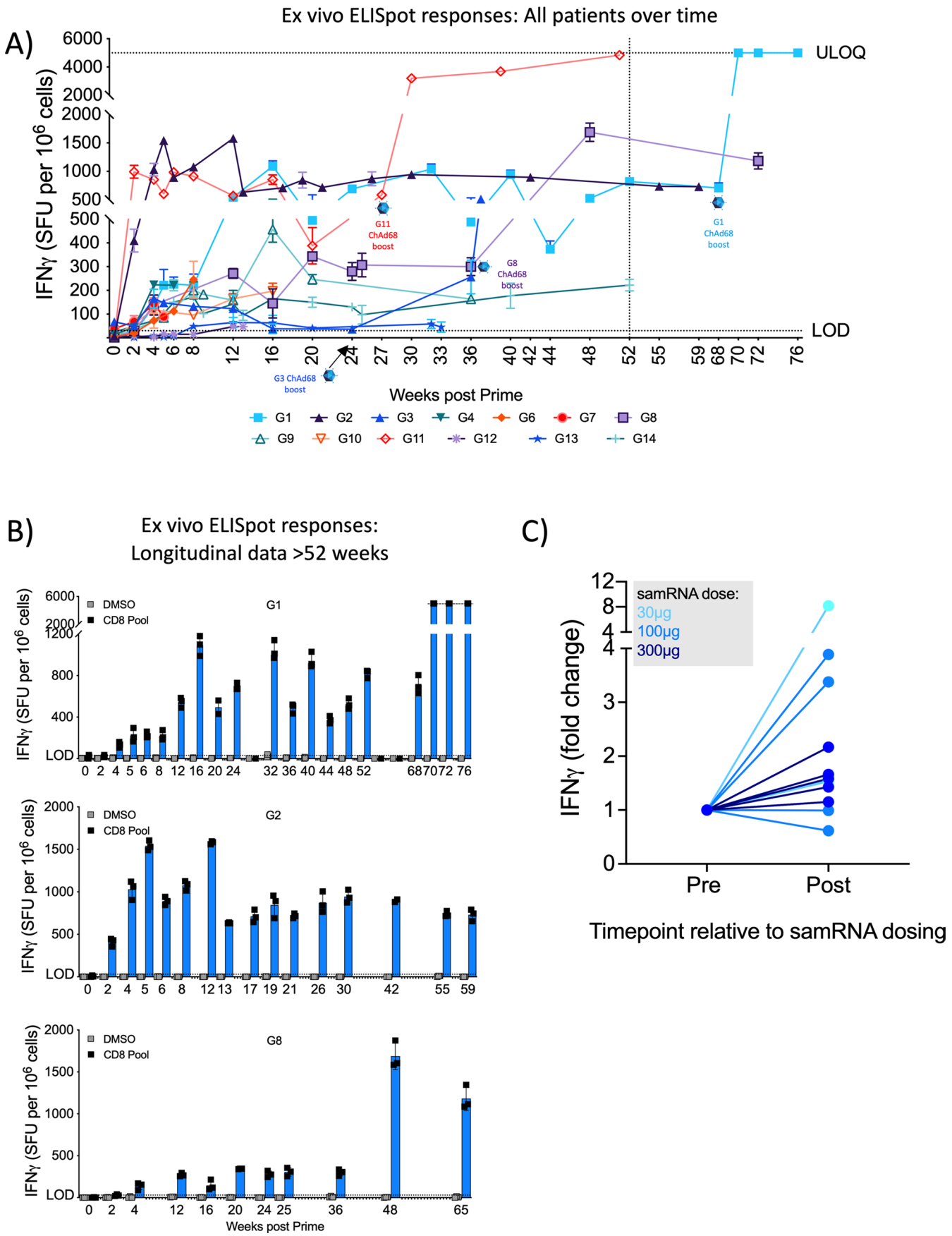

Extended Data Fig. 3 | See next page for caption.

Extended Data Fig. 3 | (**A)** Data from PBMCs stimulated overnight in *ex vivo* IFNγ ELISpot with patient-specific peptide pools are shown for all Phase patients with available samples (all except G5). Individual patient IDs legend is shown below graph. Graphs show mean SFU per 10^6 PBMCs +/- standard deviation (SD) for technical triplicates (ELISpot wells) for all patients and timepoints except for G1 (W20 and W72), G2 (W42), G3 (W0, W5 and W8), G6 (all timepoints), G12 (W12 and W13), G13 (W12), and G14 (all timepoints), where only sufficient cells to test technical duplicates were available. For patient G3 W1 enough cells were available to test a single well. Assay limit of detection (LOD) and upper limit of quantitation (ULOQ) are indicated by dotted lines. ChAd68 boost for patients G1, G3, G8, and G11 are indicated by adenovirus symbol. (**B)** Longitudinal ELISpot data ≥52 weeks from PBMCs stimulated overnight in *ex vivo* IFNγ ELISpot with patient-specific CD8 Pools (blue bars) or DMSO (gray bars) are shown for patients G1, G2 and G8. Graphs show mean SFU per 10^6 PBMCs +/- standard deviation (SD) for triplicate ELISpot wells. (**C)** ELISpot data (fold change of mean of technical triplicates (all except for G6 (pre and post), G12 & G13 (post), where enough cells to test duplicates were available) are shown for all patients relative to pre-samRNA boost timepoint (week 4, available for all patients except G9), and maximum response post samRNA boost (5-36 week timepoints). Graphs show paired data from patients receiving 30μg samRNA (light blue), 100μg samRNA (medium blue), and 300μg samRNA (navy blue).

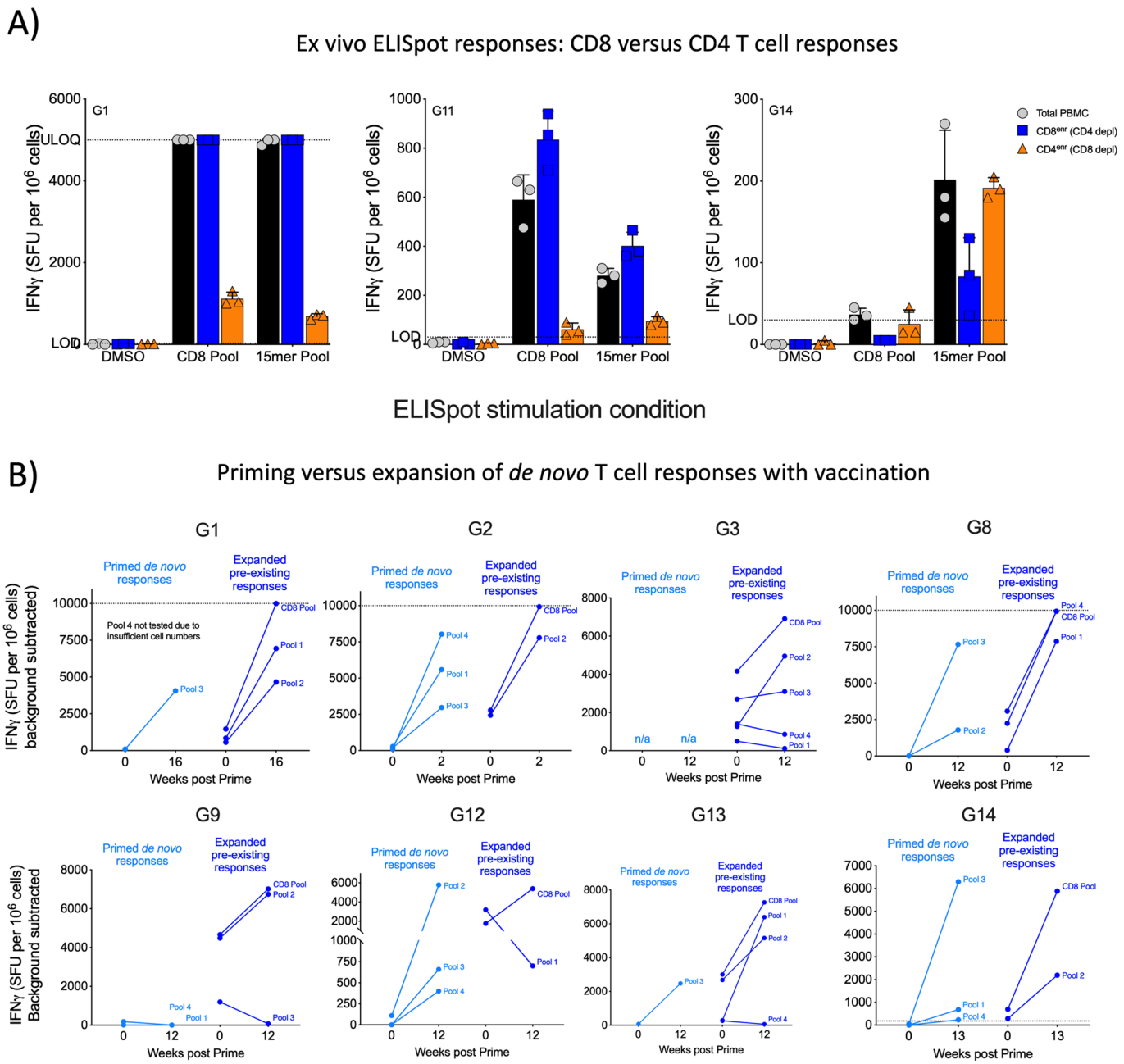

Extended Data Fig. 4 | (**A**) ELISpot data (mean SFU per 10^6 PBMCs +/- SD for triplicate wells) are shown for whole PBMCs (black bars), CD4-depleted ($CD8^{enr}$) PBMCs (navy blue bars), and CD8-depleted ($CD4^{enr}$) PBMCs (orange bars) stimulated with DMSO, CD8 Pool, or 15mer pool for patients G1, G11, and G14 (pooled posttreatment timepoints). (**B**) Post-IVS ELISpot data for baseline and posttreatment sample PBMCs stimulated with patient-specific CD8 and minipools are shown for patients G1, G2, G3, G8, G9, G12, G13 and G4. Graphs show mean of technical duplicates (SFU per 10^6 PBMCs) for all except G2 CD8 Pool, where enough cells to test triplicates were available, with DMSO background subtracted. ULOQ for post-IVS assay is indicated by dotted line.

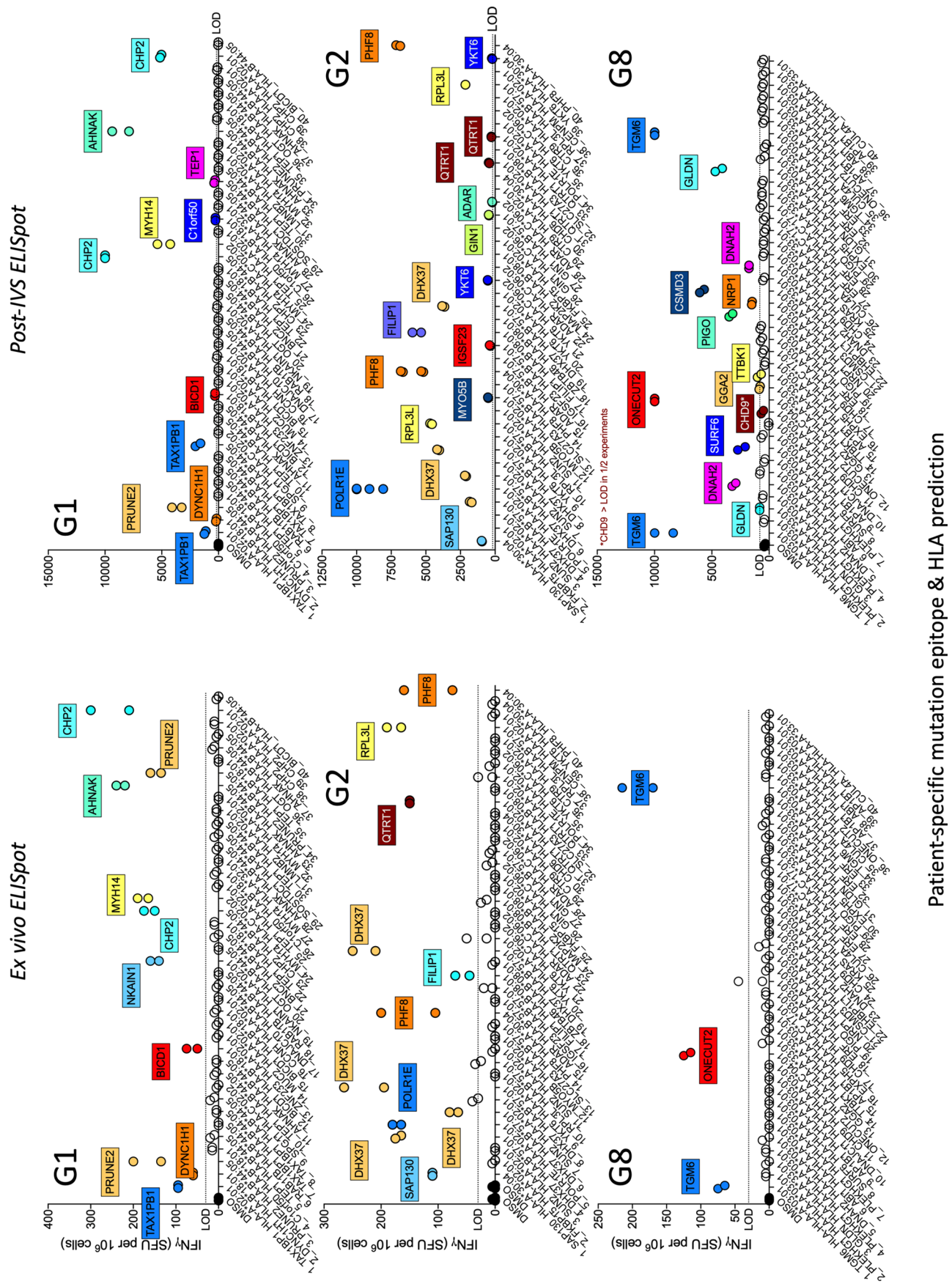

Extended Data Fig. 5 | See next page for caption.

Extended Data Fig. 5 | Data from PBMCs stimulated overnight in *ex vivo* (left graphs) or post-IVS (right graphs) IFNγ ELISpot with individual patient-specific peptides are shown for patient G1, G2, and G8. Graphs show individual duplicate values (SFU per 10^6 PBMCs) for each stimulation condition. Individual peptides with average responses >LOD (positive response) are shown in color (see mutation-specific coloring in graphs), and responses <LOD (negative response) are shown in clear circles.

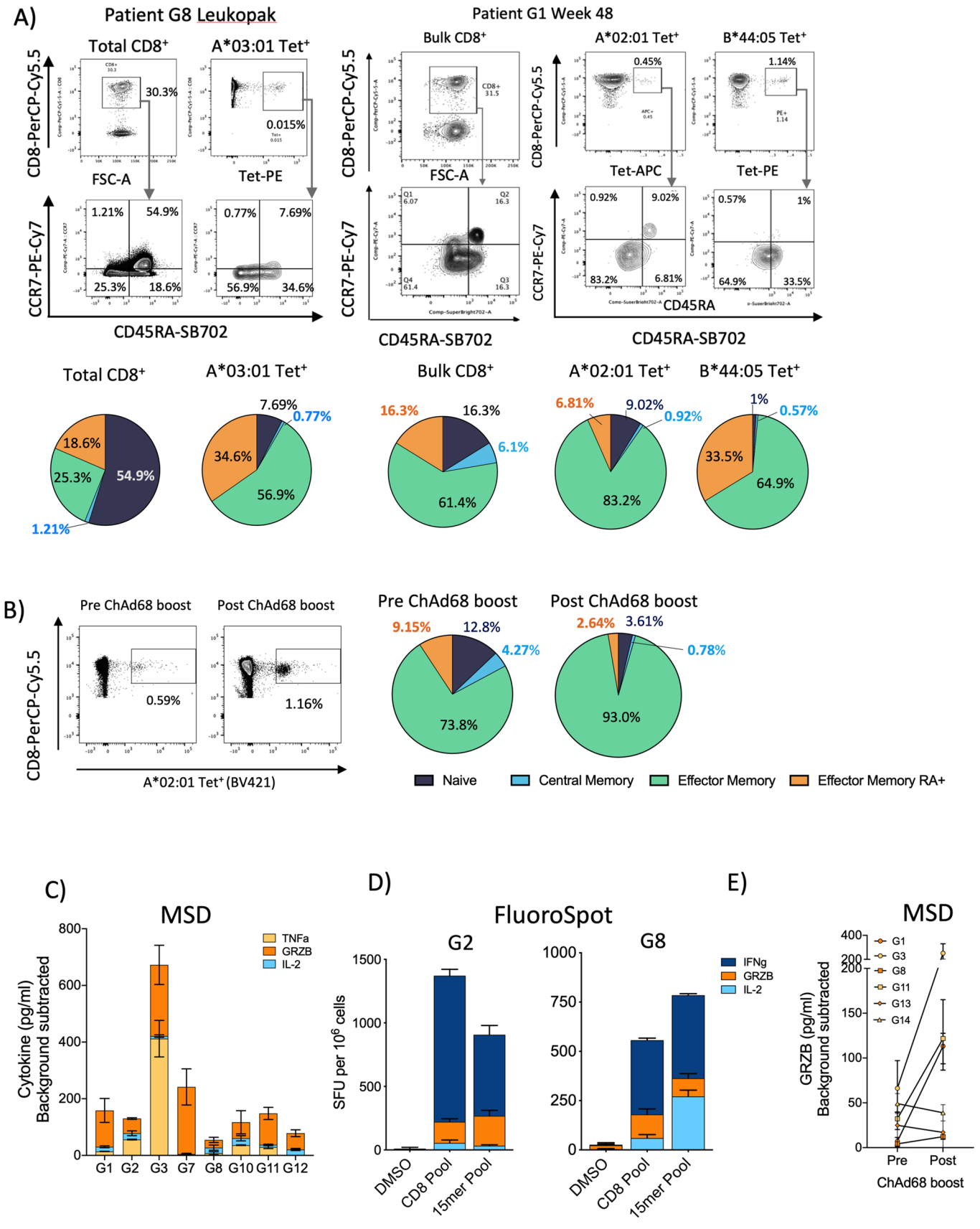

Extended Data Fig. 6 | See next page for caption.

Extended Data Fig. 6 | (**A)** Density plots showing recognition of pHLA and memory phenotypes in PBMCs from posttreatment timepoints (G1, W48, HLA-A*02:01-APC and HLA-B*44:05-PE; G8, W25, A*03:01). Pie charts showing frequencies of naïve ($CD45RA^+CCR7^+$; purple), central memory (CM; $CD45RA^-CCR7^+$; blue), effector memory (EM; $CD45RA^-CCR7^-$; green), and T effector memory RA^+ (TEMRA; $CD45RA^+CCR7^-$; orange) cells in bulk CD8 and $CD8^+$tetramer$^+$ populations from corresponding dot plots. (**B)** Density plots showing recognition of peptide-HLA (HLA-A*02:01-APC) pre- and post- ChAd68 boost for patient G1. Pie charts showing frequencies of naïve ($CD45RA^+CCR7^+$; purple), central memory (CM; $CD45RA^-CCR7^+$; blue), effector memory (EM; $CD45RA^-CCR7^-$; green), and T effector memory RA^+ (TEMRA; $CD45RA^+CCR7^-$; orange) cells in $CD8^+$tetramer$^+$ populations from corresponding dot plots. Cells were gated on lymphocytes (SSC-A vs FSC-A), single cells (FSC-H vs FSC-A), viable cells (FSC-A vs LD-AF488), $CD3^+$ cells (FSC-A vs CD3-BV421), $CD8^+Tet^+$ (CD8-PerCP-Cy5.5 vs tetramer-PE or tetramer-APC), memory phenotypes (CD45RA-SB702 vs CCR7-PE-Cy7). (**C)** Supernatants from *ex vivo* IFNγ ELISpot (G1 W5, G2 W12, G3 W37, G7 W5, G8 W12, G10 W16, G11 W2, G12 W8) were analysed by MSD U-plex assay for levels of IL-2, TNFα, and Granzyme B (GRZB) following stimulation with patient-specific CD8 Pools or DMSO. Stacked bar graphs show mean cytokine levels (triplicate wells) in pg/ml (background subtracted) +/- SD for replicate wells for IL-2 (light blue), GRZB (orange), and TNFα (yellow). (**D)** PBMCs from optional leukopak donations (G2 W19, G8 W25) were analysed by *ex vivo* FluoroSpot assay to measure IFNγ, GRZB and IL-2 expression following overnight stimulation with DMSO or patient-specific CD8 Pools. Graphs show mean SFU per 10^6 PBMCs +/- SD for triplicate FluoroSpot wells stacked for IFNγ (navy blue), GRZB (orange), and IL-2 (light blue). **E)** MSD U-plex analysis of Granzyme B (GRZB) levels in ELISpot supernatants pre- and post-ChAd68 boost for patients G1, G3, G8, G11, G13 and G14 are shown in pg/ml (background subtracted, mean +/- SD for triplicate wells). No post ChAd68-boost samples were available for patients G9 and G12.

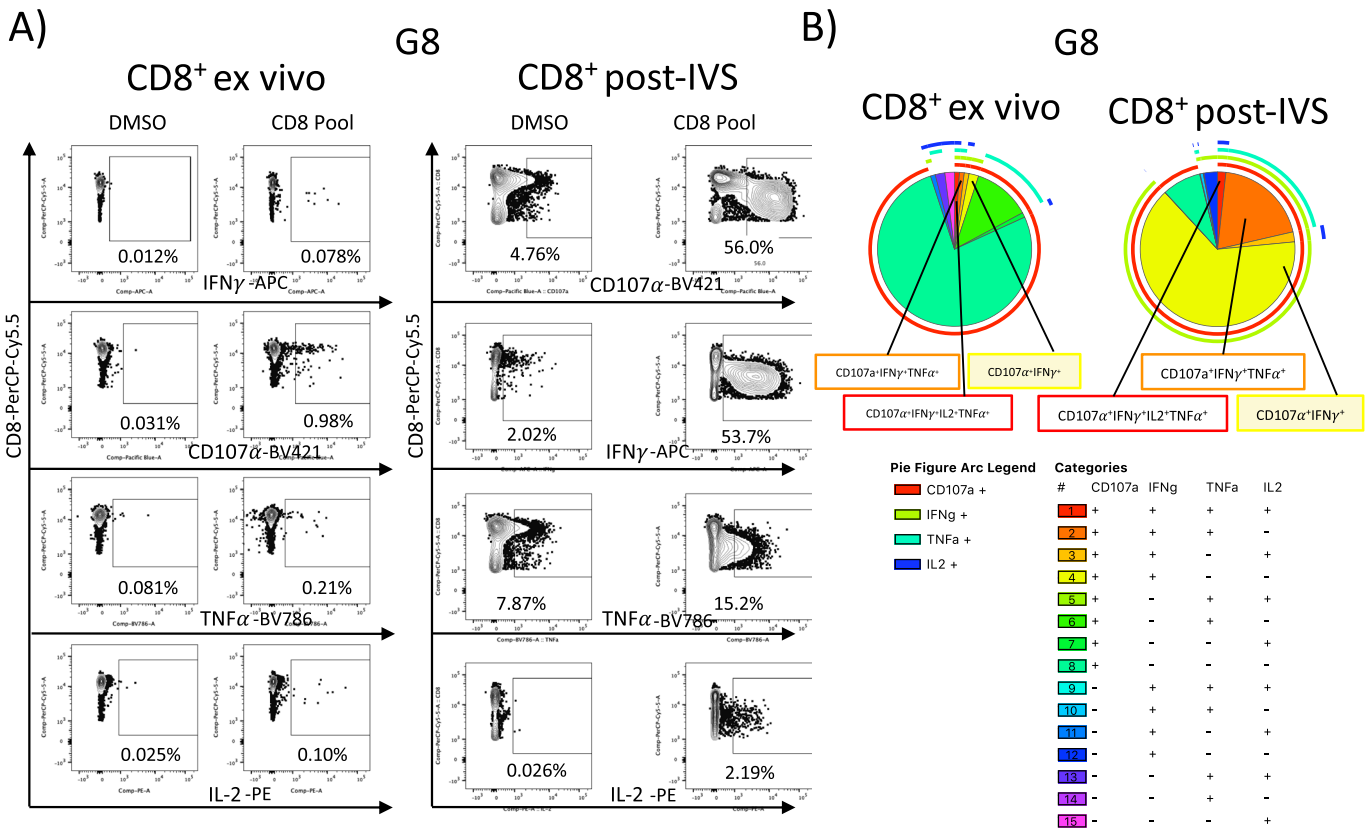

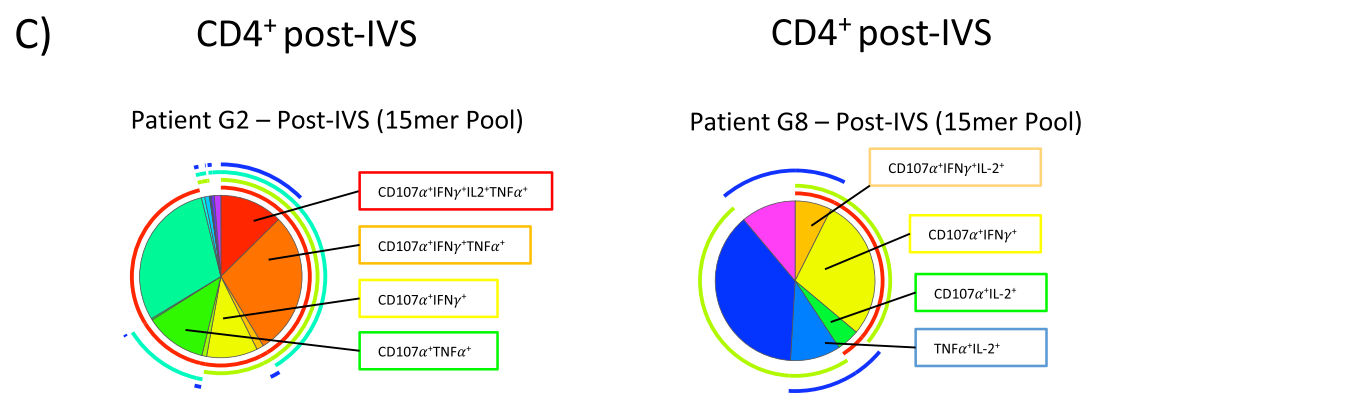

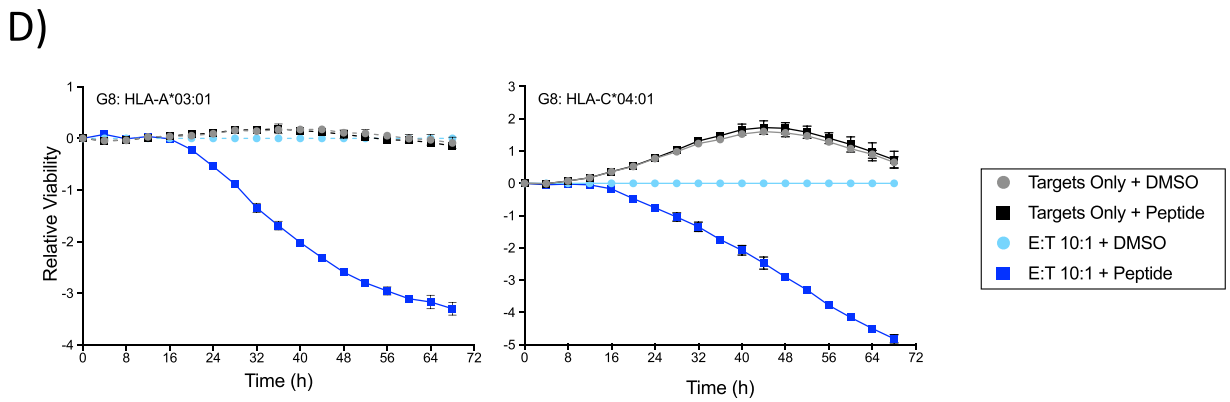

Extended Data Fig. 7 | See next page for caption.

Extended Data Fig. 7 | (**A)** Representative density plots for intracellular cytokine staining (ICS) of patient G8 *ex vivo* and IVS-expanded leukopak PBMCs stimulated overnight with either DMSO or patient-specific CD8 Pool (Supplementary Table 2) to assess production of IFNγ, CD107α, TNFα, and IL-2 in $CD8^+$ T cells. Cells were gated on PBMCs (FSC-A vs SSC-A), singlets (FSC-A vs FSC-H), live cells (FSC-A vs Live/Dead), CD8 T cells and $cytokine^+$ cells. (**B)** Polyfunctionality was assessed via Boolean gating of $CD8^+cytokine^+$ populations (background subtracted). Pie charts show polyfunctionality of *ex vivo* PBMCs (left pie chart) and post-IVS PBMCs (right pie chart). Pie arcs depict individual cytokines in red (CD107α), lime green (IFNγ), turquoise (TNFα), and navy blue (IL-2). Pie sections depict frequencies of cells expressing multiple cytokines as outlined in Pie Category legend. Main functional pie slices are colored red (quadruple positive for CD107α, IFNγ, TNFα, and IL-2), orange (triple positive for CD107α, IFNγ, and TNFα), and yellow (double positive for CD107α and IFNγ). **(C)** Polyfunctionality was assessed via Boolean gating of $CD4^+cytokine^+$ populations (background subtracted). Pie charts show polyfunctionality of post-IVS PBMCs for patient G2 (left pie chart) and G8 (right pie chart). Pie arcs depict individual cytokines in red (CD107α), lime green (IFNγ), turquoise (TNFα), and navy blue (IL-2). Pie sections depict frequencies of cells expressing multiple cytokines as outlined in Pie Category legend. Main functional pie slices are colored red (quadruple positive for CD107α, IFNγ, TNFα, and IL-2), orange (triple positive for CD107α, IFNγ, and TNFα), and yellow (double positive for CD107α and IFNγ). **(D)** Target cell killing by IVS-expanded PBMCs from patients G8 (A*03:03, C*04:01). Graphs show relative viability based on NucRed count and normalized to effector:target (E:T) ratio of 10:1 DMSO control over time. Data are shown as mean +/- SD from duplicate wells for targets alone stimulated with DMSO (gray circles) or cognate peptide (black squares), and for 10:1 E:T co-cultures stimulated with DMSO (light blue circles) or cognate peptide (navy blue squares).

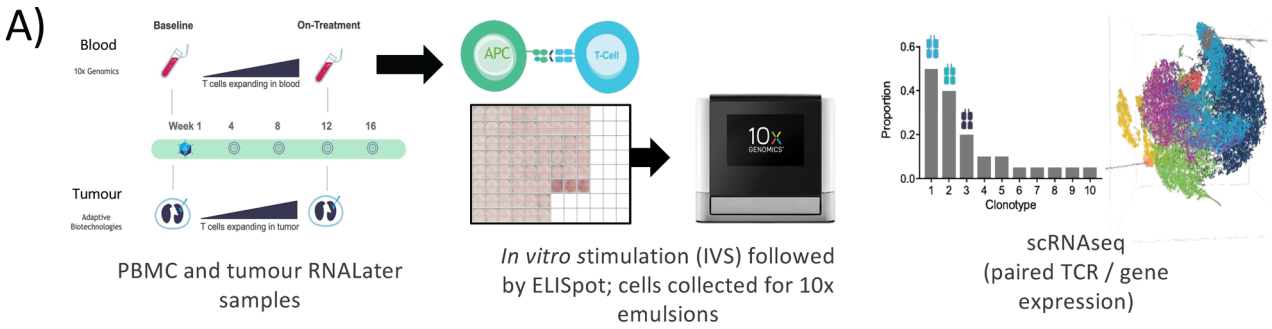

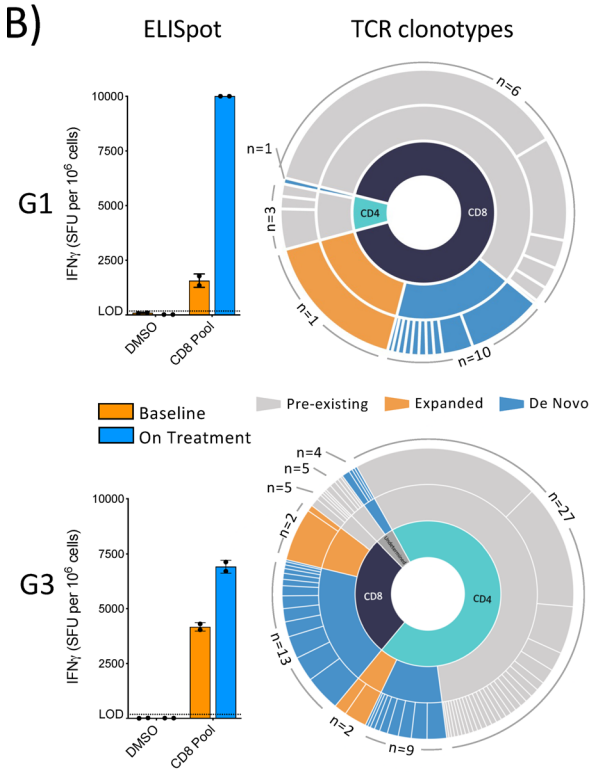

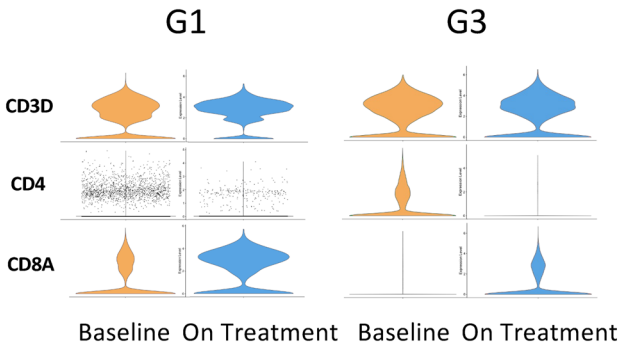

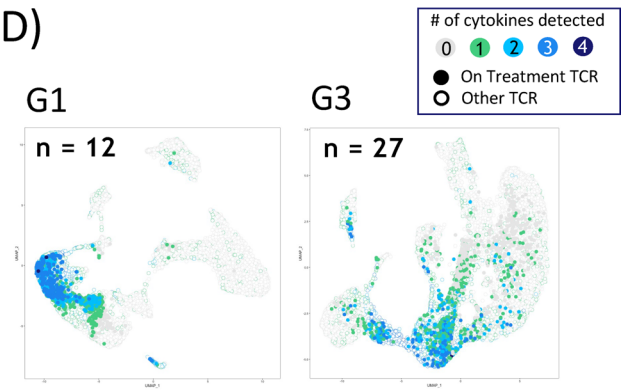

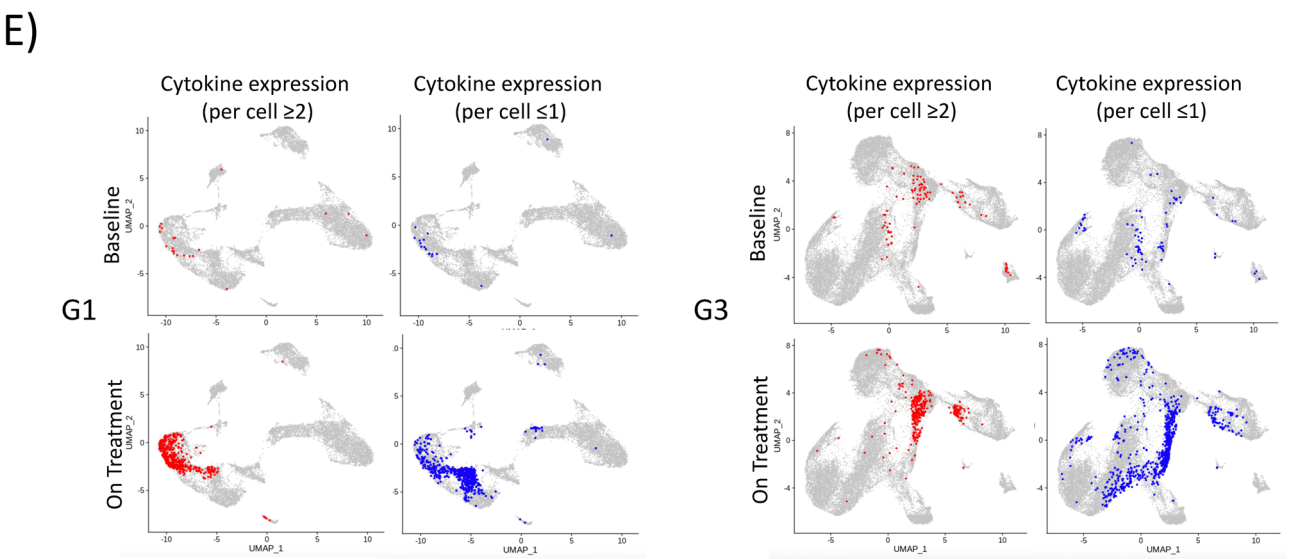

Extended Data Fig. 8 | See next page for caption.

Extended Data Fig. 8 | (**A)** Schematic outlining approach for matched PBMC and FFPE tumor tissue TCR analyses. (**B)** Post-IVS ELISpot (mean SFU per 10^6 PBMCs +/- SD for duplicate wells) from baseline (W0; orange) and on-treatment (W16; blue) timepoints corresponding to available on-treatment tumor biopsy samples (W16) for patients G1 and G3. TCR clonotypes (paired α-β chains) present at baseline and expanded on-treatment (expanded; orange) or absent at baseline and present on-treatment (*de novo* primed; blue) and the corresponding single-cell mRNA signatures for CD4 or CD8 expression are shown. Patient G1: CD8 expanded (n=1), CD8 de novo (n=10), CD8 preexisting (n=60, CD4 expanded (n=0), CD4 de novo (n=1), CD4 preexisting (n=3). Patient G3: CD8 expanded (n=2, CD8 de novo (n=13), CD8 preexisting (n=5), CD4 expanded (n=2), CD4 de novo (n=9), CD4 preexisting (n=27), undetermined expanded (n=0), undetermined de novo (n=4), undetermined preexisting (n=5). (**C)** Violin plots showing analyses of CD3, CD4, and CD8 mRNA expression in cells from baseline (orange) and on-treatment (blue) PBMC samples for patients G1 and G3. (**D)** UMAP plots showing individual cells expressing TCR clonotypes present in on-treatment samples (closed circles, n=12 for G1, n=27 for G3) and expressing 0, 1, 2, 3, or 4 cytokine transcripts (see also Supplementary Table 3). (**E)** UMAP plots showing individual cells expressing ≤1 (blue) and ≥2 cytokines (red) and TCR clonotypes of interest (n=12 for G1, n=27 for G3) comparing baseline and on-treatment samples (see also Supplementary Table 3).

Extended Data Table 1 | Listing of patient baseline characteristics, Disposition, and Efficacy by DL (as of 31 January 2022)

Dose Level (DL) [1]	Patient ID	Tumour Type	Number of prior lines of therapy	Months since diagnosis of metastatic disease	Sex	Age (years)	ECOG	Time[2] of Boost ChAd68	BOR[3]	Progression free survival[4] (Days)	Overall Survival[5] (Days)	Reason for Discontinued treatment
DL 1	G1*	GEA	1	7	M	74	0	68	SD	184	596 (died)	Completed
DL 1	G2	GEA	1	10	M	59	0	n/a	NE	939	939(alive)	Physician Decision
DL 1	G3	NSCLC	2	12	F	72	1	36	PD	53	521 (alive)	Progressive Disease
DL 2	G4	CRC	2	21	F	76	0	n/a	PD	43	169 (died)	Progressive Disease
DL 2	G5	GEA	1	9	M	63	1	n/a	PD	32	53 (died)	Death
DL 3	G6	CRC	2	36.5	M	50	1	n/a	PD	117	261 (died)	Progressive Disease
DL 3	G7	GEA	1	10	M	53	1	n/a	NE	116	116 (died)	Death
DL 3	G8*	CRC	2	24	F	51	0	36	SD	457	554 (alive)	Progressive Disease
DL 4	G9*	CRC	2	23	M	61	1	24	SD	169	262 (died)	Death
DL 4	G10*	CRC	2	18	F	38	0	n/a	PD	57	235 (died)	Progressive Disease
DL 4	G11	CRC	2	23	M	50	1	27	SD	287	491 (alive)	Progressive Disease
DL 4	G12*	GEA	1	8	M	59	1	24	PD	57	201 (died)	Progressive Disease
DL 4	G13	GEA	1	8	M	59	0	32	CR[6]	470	470 (alive)	N/A
DL 4	G14	CRC	2	23	M	48	0	24	PD	163	464 (alive)	Progressive Disease

GEA: Gastroesophageal adenocarcinoma; NSCLC: Non-Small Cell Lung Cancer; CRC: Colorectal Cancer; [1]Dose Level 1=GRT-C901/GRT-R902 30µg+ Nivolumab; Dose Level 2= GRT-C901/GRT-R902 100µg+ Nivolumab; Dose Level 3= GRT-C901/GRT-R902 100µg+ Nivolumab+ SC Ipilimumab; Dose Level 4= GRT-C901/GRT-R902 300µg+ Nivolumab+ SC Ipilimumab [2]Weeks from the prime ChAd68 dosing [3]Best of response as per RECIST v 1.1; CR=confirmed response; PR=partial response; SD=stable disease (≥ 16 weeks on treatment); PD=progressive disease; NE=no evidence of disease [4]Time from the first dose with GRT-C901 (or GRT-R902 if patient does not receive GRT-C901) to the earliest date of PD or death by any cause [5]Time to death (died) or last contact/assessment (alive) from the 1st study treatment [6]This is a confirmed complete response defined as disappearance of target liver lesions and no visible disease on imaging; biopsy at original primary tumor site showed microscopic invasive adenocarcinoma at 4 months; response duration of 6 months followed by worsening of primary esophageal lesion with dysphagia *Concurrent chemotherapy with study treatment: Patient G1 received 3 doses of 5-FU over the first 8 weeks. Patient G8 received 5-FU/bevacizumab (had been receiving for 21 months prior to study treatment). Patient G9 received FOLFIRI/cetuximab (receiving for 11 months prior to study treatment). Patient G10 received FOLFIRI (receiving for 11 months prior to study treatment). Patient G12 received Paclitaxel/ramucirumab started after 12 weeks of study treatment.

nature portfolio

Corresponding author(s): Karin Jooss

Last updated by author(s): 2022-JUN-15

Reporting Summary

Nature Portfolio wishes to improve the reproducibility of the work that we publish. This form provides structure for consistency and transparency in reporting. For further information on Nature Portfolio policies, see our Editorial Policies and the Editorial Policy Checklist.

Statistics

For all statistical analyses, confirm that the following items are present in the figure legend, table legend, main text, or Methods section.

n/a	Confirmed
☐	☒ The exact sample size (*n*) for each experimental group/condition, given as a discrete number and unit of measurement
☐	☒ A statement on whether measurements were taken from distinct samples or whether the same sample was measured repeatedly
☐	☒ The statistical test(s) used AND whether they are one- or two-sided *Only common tests should be described solely by name; describe more complex techniques in the Methods section.*
☒	☐ A description of all covariates tested
☒	☐ A description of any assumptions or corrections, such as tests of normality and adjustment for multiple comparisons
☐	☒ A full description of the statistical parameters including central tendency (e.g. means) or other basic estimates (e.g. regression coefficient) AND variation (e.g. standard deviation) or associated estimates of uncertainty (e.g. confidence intervals)
☒	☐ For null hypothesis testing, the test statistic (e.g. *F*, *t*, *r*) with confidence intervals, effect sizes, degrees of freedom and *P* value noted *Give P values as exact values whenever suitable.*
☒	☐ For Bayesian analysis, information on the choice of priors and Markov chain Monte Carlo settings
☒	☐ For hierarchical and complex designs, identification of the appropriate level for tests and full reporting of outcomes
☒	☐ Estimates of effect sizes (e.g. Cohen's *d*, Pearson's *r*), indicating how they were calculated

Our web collection on statistics for biologists contains articles on many of the points above.

Software and code

Policy information about availability of computer code

Data collection	BD FACSDiva software (BD Biosciences) Attune NxT flow cytometry software (Thermo Fisher Scientific) AID ELISpot reader software (Autoimmun Diagnostika GmbH, Straßberg, Germany) DISCOVERY WORKBENCH software (Meso Scale Discovery Inc., Rockville, MD, USA) HiSeq Software Suite (Illumina) NovaSeq Control Software (IIIlumina)
Data analysis	GraphPad Prism (GraphPad Software LLC, Version 9.0.1.) SPICE 6 (https://niaid.github.io/spice/) FlowJo (BD, Version 10.6.1.) Loupe Cell Browser (10x Genomics, Version 3.0.0.) Loupe VDJ Browser (10x Genomics, Version 3.0.0.) Incucyte® S3 Software Essen Biosciences, Satorius) fgbio (github, http://fulcrumgenomics.github.io/fgbio/tools/latest/) Samtools v1.3 (Li et al., 2009, http://www.htslib.org/) Picard v2.7.1 (github, https://broadinstitute.github.io/picard/) FreeBayes v1.0.0 (http://arxiv.org/abs/1207.3907, https://github.com/freebayes/freebayes) bwa v0.7.13 (http://arxiv.org/abs/1303.3997, http://bio-bwa.sourceforge.net/)

For manuscripts utilizing custom algorithms or software that are central to the research but not yet described in published literature, software must be made available to editors and reviewers. We strongly encourage code deposition in a community repository (e.g. GitHub). See the Nature Portfolio guidelines for submitting code & software for further information.

Data

Policy information about availability of data

All manuscripts must include a data availability statement. This statement should provide the following information, where applicable:

- Accession codes, unique identifiers, or web links for publicly available datasets
- A description of any restrictions on data availability
- For clinical datasets or third party data, please ensure that the statement adheres to our policy

De-identified individual participant clinical data that underlie the results reported in this article are available for transfer. Interested investigators can obtain and certify the data transfer agreement (DTA) and submit requests to the principal investigator K.J. Investigators and institutions who consent to the terms of the DTA form, including, but not limited to, the use of these data for the purpose of a specific project and only for research purposes, and to protect the confidentiality of the data and limit the possibility of identification of participants in any way whatsoever for the duration of the agreement, will be granted access. Gritstone will then facilitate the transfer of the requested de-identified data. This mechanism is expected to be via a Gritstone Secure File Transfer Service, but Gritstone reserves the right to change the specific transfer method at any time, provided appropriate levels of access authorization and control can be maintained. Source data are provided with this paper. Pan-Cancer Atlas (PANCAN) data sets were obtained from the cBioPortal (https://www.cbioportal.org/) and from the UCSC Xena TCGA Pan-Cancer Atlas data hub (https://pancanatlas.xenahubs.net) and raw data is available through the Genomic Data Commons (https://gdc.cancer.gov/). Epitope selection and patient-specific neoantigen selection utilized a previously published algorithm (Bulik-Sullivan et al., Nature Biotechnology, 2018).

Field-specific reporting

Please select the one below that is the best fit for your research. If you are not sure, read the appropriate sections before making your selection.

☒ Life sciences ☐ Behavioural & social sciences ☐ Ecological, evolutionary & environmental sciences

For a reference copy of the document with all sections, see nature.com/documents/nr-reporting-summary-flat.pdf

Life sciences study design

All studies must disclose on these points even when the disclosure is negative.

Sample size	14 patients
Data exclusions	No PBMC time points were available for patient G5 - no immunogenicity data are available for this patient.
Replication	Assays were performed with technical replicates. All attempts at replication were successful.
Randomization	No randomization was performed for this first-in-human phase 1/2 study.
Blinding	Investigators were not blinded to study treatment.

Reporting for specific materials, systems and methods

We require information from authors about some types of materials, experimental systems and methods used in many studies. Here, indicate whether each material, system or method listed is relevant to your study. If you are not sure if a list item applies to your research, read the appropriate section before selecting a response.

Materials & experimental systems

n/a	Involved in the study
☐	☒ Antibodies
☐	☒ Eukaryotic cell lines
☒	☐ Palaeontology and archaeology
☐	☒ Animals and other organisms
☐	☒ Human research participants
☐	☒ Clinical data
☒	☐ Dual use research of concern

Methods

n/a	Involved in the study
☐	☐ ChIP-seq
☐	☒ Flow cytometry
☐	☐ MRI-based neuroimaging

Antibodies

Antibodies used

CD3 SP34.2 A700 BD #557917
CD4 L200 PE BD #550630
CD8 SK1 APC-Cy7 BD #557834
IFNg B27 APC-R700 BD #564981

TNFa MAb11 BV421 BD # 562783
CD45RA 5H9 FITC BD #556626
CCR7 3D12 PECy7 BD #557648
CD8 SK1 e450 eBioscience #48-0087-42
CCR7 3D12 SB780 eBioscience #78-1979-42
PerCP/Cyanine5.5 anti-human CD8a Antibody BioLegend 301032
Alexa Fluor® 647 anti-human IFN-γ Antibody BioLegend 502516
CD4 Monoclonal Antibody (RPA-T4), APC-eFluor 780 Antibody eBioscience 47-0049-42
Brilliant Violet 421™ anti-human CD107a (LAMP-1) Antibody BioLegend 328625
Brilliant Violet 605™ anti-human CD3 Antibody BioLegend 317322
CD45RA Monoclonal Antibody (HI100), Super Bright 702, Antibody eBioscience 67-0458-42
Brilliant Violet 785™ anti-human TNF-α Antibody BioLegend 502948
PE anti-human IL-2 Antibody BioLegend 500307
PE/Cyanine7 anti-human CD197 (CCR7) Antibody BioLegend 353225
Purified anti-human HLA-A,B,C antibody BioLegend 311402
Brilliant Violet 421™ anti-human CD3 antibody BioLegend 300434
Pacific Blue™ anti-human HLA-A,B,C Antibody BioLegend 311418
PE anti-human HLA-A,B,C Antibody BioLegend 311405

Validation

Validation statements:
BD: Our flow cytometry reagents can help you get reliable and consistent results due to our rigorous testing and quality control standards
Biolegend: All products sold by BioLegend Inc. comply with the requirements of ISO 13485:2016. This includes products labelled as Research Use Only (RUO) or GMP Research Use Only (GMP RUO), Analyte Specific Reagents (ASRs), and In Vitro Diagnostics (IVDs) including CE-Marked and registered products in selected countries.
eBioscience (now part of ThermoFisher Scientific): As a leading provider of high-quality, validated antibodies, our products are used by researchers around the world. https://www.thermofisher.com/us/en/home/global/forms/nature-articles-ab-reproducibility-validation-specificity.html

Eukaryotic cell lines

Policy information about cell lines

Cell line source(s)	ATCC (A375 cells)
Authentication	No authentication was performed
Mycoplasma contamination	Cells were confirmed negative for mycoplasma
Commonly misidentified lines (See ICLAC register)	n/a

Animals and other organisms

Policy information about studies involving animals; ARRIVE guidelines recommended for reporting animal research

Laboratory animals	MAMU A*01 positive rhesus macaques, 10 male, 8 female, age range 4.5-18.1 years (see Supplemental Table S1 for individual animal sex and age information).
Wild animals	Study did not involve wild animals
Field-collected samples	Study did not involve field-collected samples
Ethics oversight	Study was performed according to IACUC approved protocol at the California National Primate Research Center at the University of California at Davis.

Note that full information on the approval of the study protocol must also be provided in the manuscript.

Human research participants

Policy information about studies involving human research participants

Population characteristics	Patients with advanced or metastatic non-small cell lung cancer, gastroesophageal adenocarcinoma, metastatic urothelial carcinoma, or microsatellite stable colorectal cancer who are ≥ 18 years of age.
Recruitment	Patients were recruited at selected clinical sites across the United States of America
Ethics oversight	The protocol was reviewed and approved by an institutional review board (IRB) at each participating clinical site.

Note that full information on the approval of the study protocol must also be provided in the manuscript.

Clinical data

Policy information about clinical studies

All manuscripts should comply with the ICMJE guidelines for publication of clinical research and a completed CONSORT checklist must be included with all submissions.

Clinical trial registration	NCT03639714
Study protocol	Study protocol is available as part of the supplemental information submitted with the manuscript.
Data collection	Clinical data was collected in an electronic data capture system database based on case report forms. Patients were enrolled from February 2019 to September 2020. Immunogenicity data were generated and analyzed by the study sponsor using patient's peripheral blood mononuclear cells.
Outcomes	The primary and secondary endpoints for safety, recommended phase 2 dose, and immunogenicity were pre-defined per the protocol. The statistical analysis plan was finalized prior to primary analysis.

ChIP-seq

Data deposition

☐ Confirm that both raw and final processed data have been deposited in a public database such as GEO.

☐ Confirm that you have deposited or provided access to graph files (e.g. BED files) for the called peaks.

Data access links *May remain private before publication.*	*For "Initial submission" or "Revised version" documents, provide reviewer access links. For your "Final submission" document, provide a link to the deposited data.*
Files in database submission	*Provide a list of all files available in the database submission.*
Genome browser session (e.g. UCSC)	*Provide a link to an anonymized genome browser session for "Initial submission" and "Revised version" documents only, to enable peer review. Write "no longer applicable" for "Final submission" documents.*

Methodology

Replicates	*Describe the experimental replicates, specifying number, type and replicate agreement.*
Sequencing depth	*Describe the sequencing depth for each experiment, providing the total number of reads, uniquely mapped reads, length of reads and whether they were paired- or single-end.*
Antibodies	*Describe the antibodies used for the ChIP-seq experiments; as applicable, provide supplier name, catalog number, clone name, and lot number.*
Peak calling parameters	*Specify the command line program and parameters used for read mapping and peak calling, including the ChIP, control and index files used.*
Data quality	*Describe the methods used to ensure data quality in full detail, including how many peaks are at FDR 5% and above 5-fold enrichment.*
Software	*Describe the software used to collect and analyze the ChIP-seq data. For custom code that has been deposited into a community repository, provide accession details.*

Flow Cytometry

Plots

Confirm that:

☒ The axis labels state the marker and fluorochrome used (e.g. CD4-FITC).

☒ The axis scales are clearly visible. Include numbers along axes only for bottom left plot of group (a 'group' is an analysis of identical markers).

☒ All plots are contour plots with outliers or pseudocolor plots.

☒ A numerical value for number of cells or percentage (with statistics) is provided.

Methodology

Sample preparation	Intracellular cytokine staining (ICS) assay (NHP study) Freshly isolated PBMCs were distributed at 106 per well into v-bottom 96-well plates. Cells were pelleted and resuspended in 100µl of complete RPMI containing 1µg/ml anti-CD28 mAb (CD28.2, BD Biosciences) and 1µg/ml anti-CD49d mAb (9F10, BD Biosciences), and 10µg/ml pooled peptide antigens, or WLS antigen as a negative control stimulant (Genscript). After 1h of stimulation, Brefeldin A (Biolegend) was added to a final concentration of 5µg/ml and incubated for an additional 16h.

Following stimulation, cells were washed with PBS and stained with fixable viability dye (eBioscience). Extracellular staining was performed in FACS buffer (PBS + 2% FBS + 2mM EDTA) with anti-CD3, anti-CD4, anti-CTLA-4, anti-PD1 and anti-CD8 antibodies. Cells were washed, fixed and permeabilized with Transcription Factor fixation/permeabilization kit (eBioscience) and then intracellular staining was performed in permeabilization buffer. Samples were stained for IFN□, TNF□, Granzyme B and CD69. Samples were collected on the Attune NxT (Thermofisher). Gating strategy was as follows (see Supplemental Figure S1): Lymphocytes (SSC-A vs FSC-A), single cells (SSC-H vs SSC-A), viable cells (SSC-A vs LD-506), CD4+ or CD8+ (CD4-PE vs CD8-e450), cytokine+ (TNFa-BV421 vs IFNg-APC-R700).

Tetramer staining assay (NHP study)
Following overnight rest at 4°C, isolated PBMCs were distributed into 96-well V-bottom plates at a density of 106 cells/100µl and stained with a viability dye (Live/Dead e506, eBioscience) in PBS for 20min at 4°C. TCR recycling was inhibited by treatment with 50nM Dasatinib for 1h at 4°C. Cells were stained for 1h at 4°C in FACs buffer with Mamu-A*01 tetramers for each of the peptide antigens, with a unique combination of two fluorophores per antigen (produced in-house). Cells were co-stained for: CD3 (A700, SP34.2, BD), CD8 (e450, SK1, BD), CD45RA (FITC, 5H9, BD), CCR7 (SB780, 3D12, eBioscience). Samples were collected on the Attune NxT (ThermoFisher). Gating strategy was as follows (see Supplemental Figure S1): Lymphocytes (SSC-A vs FSC-A), single cells (SSC-H vs SSC-A), viable cells (SSC-A vs LD-506), CD3+ cells (SSC-A vs CD3-A700), CD8+ (SSC-A vs versus CD8-e450), tetramer double+ (tetramer-UV405 vs tetramer-UV605; tetramer-UV405 vs tetramer-PE; tetramer-PE vs tetramer-UV675; tetramer-PE-Cy7 vs tetramer-UV405), memory populations (CD45RA-FITC vs CCR7-SB780).

Cytotoxicity (T-cell killing) assay (NHP study)
Freshly isolated PBMCs for each sample were divided into 2 portions: T-cell enrichment was performed on one portion using the Miltenyi NHP T-cell isolation kit (Cat # 130-092-143), following manufacturer's protocol and using MS columns (Miltenyi) to deplete non-T-cells. The second portion (referred to as PBMC) was stained with CFSE at 1mM (eBioscience). The CFSE labelled PBMCs were then loaded with 50mg/ml of either SIV peptides or a negative control peptide (WLSLLVPFV) by incubation for 1h at 37℃ in RPMI + 1% FBS. Isolated T-cells and peptide-loaded PBMC target cells were then counted and plated in a 20:1 ratio (T-cells to target cells) in a V-bottom plate. 400,000 T-cells and 20,000 target cells were plated per well. Target cells only were also plated as a control. Cells were incubated for 6h at 37℃ in RPMI + 10% FBS. Following incubation, cells were stained with 7AAD (Thermo) and immediately analysed by flow cytometry using a Cytoflex LX (Beckman). CFSE+ target cells were gated and 7AAD+ cells measured (as a percent of CFSE+ cells). Remnant T-cells were also analysed by flow cytometry to confirm T-cell isolation. Samples were collected on the Attune NxT (Thermofisher). Gating strategy was as follows (see Supplemental Figure S1): Lymphocytes (SSC-A vs FSC-A), single cells (SSC-H vs SSC-A), 7-AAD+CFSE+ (7-AAD vs CFSE).

ICS (clinical study)
PBMCs or IVS-expanded PBMCs were stimulated with either cognate minimal (8-11mer) or long overlapping (15mer) peptides, DMSO (vehicle control; VWR) or PMA/Ionomycin cell stimulation cocktail (positive control; Affymetrix, Santa Clara, CA, USA) in the presence of anti-Human CD28/CD49d antibody (BD Biosciences, San Jose, CA, USA), anti-human CD107□-BV421 (BioLegend), BD GolgiStop (BD Biosciences), and Brefeldin A (BioLegend) over a period of 18h. Following overnight incubation, cells were stained with live/dead Zombie-Red (BioLegend) and surface marker antibodies (CD8-PerCP-Cy5.5, CD3-BV605, CCR7-PE-Cy7 from BioLegend; CD4-APC-eF780, CD45RA-SuperBright702 from eBioscience; PD-1-BUV737 from BD Biosciences) prior to fixation and permeabilization with FIX & PERM™ Cell Permeabilization Kit (ThermoFisher, Waltham, MA, USA). Following permeabilization, cells were stained for intracellular cytokines using anti-human IFN□-APC, TNF□-BV785, and IL-2-PE antibodies (BioLegend) prior to data acquisition on a BD LSRFortessaTM flow cytometer (BD Biosciences).

HLA Class I fluorophore-conjugated tetramer generation and staining (clinical study)
HLA Class I tetramers were generated from Flex-TTM biotinylated HLA monomers (BioLegend, San Diego, CA, USA) or MBL International (Woburn, MA, USA) with target peptides loaded onto the monomers by UV exchange according to the manufacturer's instructions. Successful loading of target peptides by UV exchange was assessed by ELISA (BioLegend, according to manufacturer's instructions). Alternatively, biotinylated monomers were generated in-house and pre-folded with target peptides. Peptide-HLA (pHLA) monomers were assembled into tetramers using fluorophore-conjugated Streptavidin (PE from BioLegend; APC from eBioscience, San Diego, CA, USA). Using generated fluorophore-labelled peptide-MHC tetramers, PBMC were tetramer stained to help identify antigen specific T cells. Patient PBMC samples were thawed and resuspended in a 96 well V bottom plate with FACs buffer (PBS, 10% FBS [v/v]). Prior to staining, samples were incubated with 50nM Dasatinib (Sigma Aldrich, St. Louis, MO, USA) in a 5% CO2, 37℃ incubator for 30min. Subsequently, HLA Class I fluorophore labelled tetramers loaded with target peptides of interest were added directly to each corresponding PBMC sample. In instances where multiple tetramers needed to be added to the same sample, a cocktail was made with equal amounts of each tetramer, then mixed and added at the same time. Samples were incubated at room temperature for 1h in the dark. Following incubation, samples were washed in FACS buffer, and stained with an antibody master mix containing purified anti-human HLA-A,B,C Antibody, anti-human CD8-PerCP-Cy5.5, anti-human CCR7-PE-Cy7, anti-human CD3-BV421 (all BioLegend), anti-human CD45RA-SB702, anti-human CD4-APC-eF780 (both eBioscience) and Live/Dead Green (ThermoFisher). Sample were mixed and incubated at 4℃ in the dark protected from light for 20min. Samples were washed once with FACs buffer and then resuspended in FACs buffer prior to acquisition on a BD LSRFortessaTM flow cytometer (BD Biosciences).

Instrument

Attune NxT (Thermofisher), BD LSRFortessaTM flow cytometer (BD Biosciences), Cell Sorter SH800S (SONY Biotechnology Inc.)

Software

BD FACSDiva software
Attune NxT flow cytometry software
Sony Cell Sorter SH800S software
FlowJo software (FlowJo, LLC, Ashland, OR, USA)
SPICE software v6

Cell population abundance	A375 The HLA null fraction was sorted (80% of population); post-sort frequency of HLA positive cells was 0%
Gating strategy	Gating strategies are outlines in Supplemental Figures S1, S2, S3, and S4. NHP studies: ICS: Gating strategy was as follows (see Supplemental Figure S1): Lymphocytes (SSC-A vs FSC-A), single cells (SSC-H vs SSC-A), viable cells (SSC-A vs LD-506), CD4+ or CD8+ (CD4-PE vs CD8-e450), cytokine+ (TNFa-BV421 vs IFNg-APC-R700). Tetramer: Gating strategy was as follows (see Supplemental Figure S1): Lymphocytes (SSC-A vs FSC-A), single cells (SSC-H vs SSC-A), viable cells (SSC-A vs LD-506), CD3+ cells (SSC-A vs CD3-A700), CD8+ (SSC-A vs versus CD8-e450), tetramer double+ (tetramer-UV405 vs tetramer-UV605; tetramer-UV405 vs tetramer-PE; tetramer-PE vs tetramer-UV675; tetramer-PE-Cy7 vs tetramer-UV405), memory populations (CD45RA-FITC vs CCR7-SB780). Cytotoxicity: Gating strategy was as follows (see Supplemental Figure S1): Lymphocytes (SSC-A vs FSC-A), single cells (SSC-H vs SSC-A), 7-AAD+CFSE+ (7-AAD vs CFSE). Human samples: Gating strategies for human samples are as follows (see Supplemental Figures S2 and S3): CD4 versus CD8 T cell assessments: Lymphocytes (SSC-A vs FSC-A), single cells (FSC-H vs FSC-A), viable cells (FSC-A vs LD-ZombieRed), CD3+ cells (FSC-A vs CD3-BV605), CD4+ and CD8+ (CD4-APCeF780 vs CD8-PerCP-Cy5.5). Tetramer studies: Lymphocytes (SSC-A vs FSC-A), single cells (FSC-H vs FSC-A), viable cells (FSC-A vs LD-AF488), CD3+ cells (FSC-A vs CD3-BV421), CD8+Tet+ (CD8-PerCP-Cy5.5 vs tetramer-PE or tetramer-APC), memory phenotypes (CD45RA-SB702 vs CCR7-PE-Cy7). ICS studies: Lymphocytes (SSC-A vs FSC-A), single cells (FSC-H vs FSC-A), viable cells (FSC-A vs LD-ZombieRed), CD3+ cells (FSC-A vs CD3-BV605), CD4+ and CD8+ (CD4-APCeF780 vs CD8-PerCP-Cy5.5), CD8+ or CD4+ cytokine+ cells (CD8-PerCP-Cy5.5 vs CD107a-BV421, IFNg-APC, TNFa-BV786, IL-2-PE; CD4-APCeF780 vs CD107a-BV421, IFNg-APC, TNFa-BV786, IL-2-PE). Polyfunctionality analyses were performed using Boolean gating (FlowJo) and graphed using SPICE software v6. Results are represented as % positive cell populations (frequency of parent). Data shown as background subtracted where indicated.

☒ Tick this box to confirm that a figure exemplifying the gating strategy is provided in the Supplementary Information.

Magnetic resonance imaging

Experimental design

Design type	*Indicate task or resting state; event-related or block design.*
Design specifications	*Specify the number of blocks, trials or experimental units per session and/or subject, and specify the length of each trial or block (if trials are blocked) and interval between trials.*
Behavioral performance measures	*State number and/or type of variables recorded (e.g. correct button press, response time) and what statistics were used to establish that the subjects were performing the task as expected (e.g. mean, range, and/or standard deviation across subjects).*

Acquisition

Imaging type(s)	*Specify: functional, structural, diffusion, perfusion.*
Field strength	*Specify in Tesla*
Sequence & imaging parameters	*Specify the pulse sequence type (gradient echo, spin echo, etc.), imaging type (EPI, spiral, etc.), field of view, matrix size, slice thickness, orientation and TE/TR/flip angle.*
Area of acquisition	*State whether a whole brain scan was used OR define the area of acquisition, describing how the region was determined.*

Diffusion MRI ☐ Used ☐ Not used

Preprocessing

Preprocessing software	*Provide detail on software version and revision number and on specific parameters (model/functions, brain extraction, segmentation, smoothing kernel size, etc.).*
Normalization	*If data were normalized/standardized, describe the approach(es): specify linear or non-linear and define image types used for transformation OR indicate that data were not normalized and explain rationale for lack of normalization.*
Normalization template	*Describe the template used for normalization/transformation, specifying subject space or group standardized space (e.g. original Talairach, MNI305, ICBM152) OR indicate that the data were not normalized.*
Noise and artifact removal	*Describe your procedure(s) for artifact and structured noise removal, specifying motion parameters, tissue signals and physiological signals (heart rate, respiration).*
Volume censoring	*Define your software and/or method and criteria for volume censoring, and state the extent of such censoring.*

Statistical modeling & inference

Model type and settings	*Specify type (mass univariate, multivariate, RSA, predictive, etc.) and describe essential details of the model at the first and second levels (e.g. fixed, random or mixed effects; drift or auto-correlation).*
Effect(s) tested	*Define precise effect in terms of the task or stimulus conditions instead of psychological concepts and indicate whether ANOVA or factorial designs were used.*

Specify type of analysis: ☐ Whole brain ☐ ROI-based ☐ Both

Statistic type for inference (See Eklund et al. 2016)	*Specify voxel-wise or cluster-wise and report all relevant parameters for cluster-wise methods.*
Correction	*Describe the type of correction and how it is obtained for multiple comparisons (e.g. FWE, FDR, permutation or Monte Carlo).*

Models & analysis

n/a	Involved in the study
☐	☐ Functional and/or effective connectivity
☐	☐ Graph analysis
☐	☐ Multivariate modeling or predictive analysis

Functional and/or effective connectivity	*Report the measures of dependence used and the model details (e.g. Pearson correlation, partial correlation, mutual information).*
Graph analysis	*Report the dependent variable and connectivity measure, specifying weighted graph or binarized graph, subject- or group-level, and the global and/or node summaries used (e.g. clustering coefficient, efficiency, etc.).*
Multivariate modeling and predictive analysis	*Specify independent variables, features extraction and dimension reduction, model, training and evaluation metrics.*